

## **ANEXO 13**

### **MÉTODO ELECTROMAGNÉTICO DE LAS IMÁGENES.**

# Calculation of Resistances to Ground

Formulas for practical use in the calculation of the resistances from grounding conductors of various forms to the earth are given in this paper and their use illustrated by examples. The accuracy of the formulas varies considerably, as discussed in the paper, but is sufficiently good that the methods should be helpful to those whose work involves problems of grounding.

By  
**H. B. DWIGHT**  
 FELLOW AIEE  
 Massachusetts Institute of Technology, Cambridge

**A**N ELECTRICAL CONNECTION to the ground requires consideration of the engineering problem of obtaining the lowest number of ohms to ground for a given cost. This problem involves the need of formulas for comparing different arrangements of ground conductors. A collection of such formulas for d-c resistance is given in this paper, with some discussion as to their relative accuracy. In order to compare 2 arrangements of conductors, it is usual to assume that they are both placed in earth of the same uniform conductivity. It is well-known that there is usually considerable variation of earth conductivity in the vicinity of ground conductors, but that effect is a separate problem.

## CYLINDRICAL CONDUCTOR

A very common type of ground connector is that of a vertical ground rod. Such a rod is an isolated cylinder and the flow of electricity from it into and through the ground is calculated by the same expressions as is the flow of dielectric flux from an isolated charged cylinder. That is, the problem of the resistance to ground of the ground rod is essentially the same as that of the capacitance of an isolated cylinder whose length is very great compared to its radius. The following formula for the latter case has been given by E. Hallén:<sup>1</sup>

$$\frac{C}{L} = \frac{1}{\lambda} + \frac{1.22741}{4\lambda^2} + \frac{2.17353}{8\lambda^3} + \frac{11.0360}{16\lambda^4} \dots$$

where  
 $\lambda = \log_e (2L/a)$   
 $2L$  = length of the isolated cylinder in centimeters  
 $a$  = radius of the cylinder in centimeters  
 $C$  = capacitance in absolute electrostatic units, or statfarads  
 $\log_e$  denotes natural logarithm

By taking unity divided by this series, an expression is obtained which is more convenient for the present purpose, and which is more rapidly convergent, to a slight extent, as follows:

$$\frac{1}{C} = \frac{1}{L} \left( \lambda - 0.306852 - \frac{0.17753}{\lambda} - \frac{0.5519}{\lambda^2} \dots \right) \quad (1)$$

This formula has been checked, and close agreement found, by a successive approximation calculation<sup>2</sup> in which uniform distribution of charge is first assumed and then other distributions of charge are successively added, so as to keep the potential of the cylinder the same throughout. The formula has been checked also by Dr. F. W. Grover<sup>3</sup> by a successive approximation method using mechanical integration.

An approximate method of calculation which is used for a great many shapes of conductors is the average potential method of Dr. G. W. O. Howe.<sup>4</sup> This consists in assuming uniform charge density over the surface of the conductor and calculating the average potential. Then the approximate capacitance is taken as equal to the total charge divided by the average potential. This method is correct within 2 or 3 parts in 1,000 for a long straight antenna wire, and within less than 1 per cent for a cylinder of the proportions of a ground rod. However, an estimate of its accuracy should be made for each shape or combination of conductors with which it is used, because in some cases it gives an error of several per cent. For example, it gives a value of  $1/C$  for a thin round plate which is 8 per cent too high (see the paragraph following equation 35).

Assuming a uniform charge density  $q$  per centimeter along the cylinder, on its curved surface, the potential at  $P$  (figure 1) because of the ring  $dy$  is, by equation 6, page 153, reference 10,

$$q \frac{dy}{a} \left[ \frac{a}{r} - \frac{1}{2} \frac{a^2}{r^2} \left( \frac{3y^2}{r^2} - 1 \right) + \dots \right] \quad (2)$$

where  $r^2 = a^2 + y^2$  and  $y$  is the distance from  $P$  to the ring.

Integrate equation 2 from  $y = 0$  to  $L - x$  and also from 0 to  $L + x$ , obtaining the potential at  $P$  resulting from the parts of the cylinder to the right and left of  $P$ . Then multiply by  $dx/L$  and integrate from  $x = 0$  to  $L$ , giving the average potential of the cylinder resulting from uniform charge density on its curved surface, as follows:

$$\frac{V_{av}}{2q} = \log_e \frac{4L}{a} - 1 + \frac{a}{L} \left( \frac{1}{2} + \frac{1}{8} + \frac{1}{128} + \dots \right) - \frac{a^2}{L^2} \left( \frac{3}{16} - \frac{1}{32} \dots \right) + \frac{a^4}{L^4} \left( \frac{1}{64} - \frac{1}{1024} \dots \right) \quad (3)$$

$$\frac{1}{C} = \frac{V_{av}}{2qL} = \frac{1}{L} \left( \log_e \frac{4L}{a} - 1 + 0.63 \frac{a}{L} - 0.16 \frac{a^2}{L^2} + 0.015 \frac{a^4}{L^4} \dots \right) \quad (4)$$

A paper recommended for publication by the AIEE committee on power transmission and distribution. Manuscript submitted July 22, 1936; released for publication September 4, 1936.

1. For all numbered references see list at end of paper.

If, as is often done, only the first term of equation 5 is used, the result is

$$\frac{1}{C} = \frac{1}{L} \left( \log_e \frac{2L + \sqrt{a^2 + 4L^2}}{a} + \frac{a}{2L} - \sqrt{1 + \frac{a^2}{4L^2}} \right) \quad (5)$$

which, when expanded, becomes

$$\frac{1}{C} = \frac{1}{L} \left( \log_e \frac{4L}{a} - 1 + 0.5 \frac{a}{L} - 0.06 \frac{a^2}{L^2} + 0.002 \frac{a^4}{L^4} \dots \right) \quad (6)$$

It may be seen that equation 6 does not have the right coefficients for terms in  $a/L$  and so equations 6 and 5 should not be used. For long cylinders of the proportions of wires or vertical ground rods, the

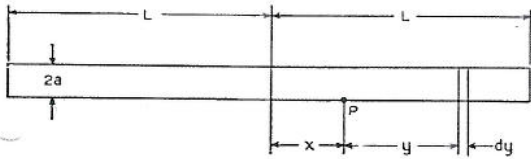


Fig. 1 (above). Cylindrical conductor

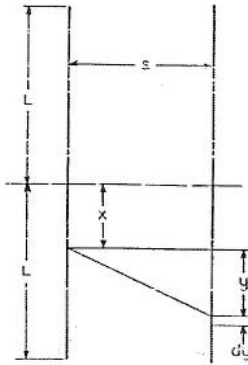


Fig. 2 (left). Two rods connected in parallel

terms in  $a/L$  and its powers are of very small effect and may be omitted, thus giving the practical formula

$$\frac{1}{C} = \frac{1}{L} \left( \log_e \frac{4L}{a} - 1 \right) \quad (7)$$

This gives an error of less than one per cent in practical cases of resistance to ground. The error is due to the approximation inherent in the average potential method and if a more accurate formula is desired, equation 1 should be used. The small error in equation 7 cannot be avoided by including terms in  $a/L$  or by using more complicated expressions in logarithms or inverse hyperbolic functions such as equation 5 or its equivalent forms.

The formula

$$\frac{1}{C} = \frac{1}{L} \log_e \frac{2L}{a} \quad (8)$$

which is based on the capacitance of an ellipsoid of revolution of the same diameter and length as the

cylinder, has a larger error than equation 7, and should not be used. Logarithms to base 10 may be used, by noting that  $\log_e p = 2.303 \log_{10} p$ .

The method of changing a formula for capacitance into one for resistance to ground, or through the ground, may be found by considering the simple case of 2 parallel plates whose distance apart is small and the effect of whose edges may be neglected.

If each of the 2 plates has an area of  $B$  square centimeters and if the charge density on one is  $q$  per square centimeter and that on the other  $-q$  per square centimeter, the number of lines of dielectric flux through air from one plate to the other is  $4\pi qB$ . The volts per centimeter in the space between the plates is equal to  $4\pi q$ , the density of the lines, and the potential difference  $V$  between the plates is  $4\pi qs$ , where the separation of the plates is  $s$  centimeters. Then

$$\frac{1}{C} = \frac{V}{qB} = \frac{4\pi s}{B} \quad (9)$$

For the flow of electricity between the same plates when they are embedded in earth of resistivity  $\rho$  abohms per centimeter cube, the resistance between the plates in abohms is

$$R = \frac{\rho s}{B} \quad (10)$$

Thus in this case,

$$R = \frac{\rho}{4\pi C} \quad (11)$$

where  $C$  is in statfarads. If  $\rho$  is in ohms per centimeter cube,  $R$  will be in ohms. Equation 11 shows merely the relation between the units and has nothing to do with the geometry of the flow of dielectric flux and current which in equations 9 and 10 is represented by the letters  $s/B$ . Equation 11 applies to any conductor or combination of conductors (see reference 11, appendix III, page 219).

The resistance of a buried straight wire of length  $2L$  centimeters, no part of which is near the surface of the ground, is given by equations 7 and 11 and is

$$R = \frac{\rho}{4\pi L} \left( \log_e \frac{4L}{a} - 1 \right) \quad (12)$$

A vertical ground rod which penetrates to a depth of  $L$  centimeters must be considered along with its image in the ground surface. The voltage and the shape of current flow are the same as for a completely buried cylinder of length  $2L$  centimeters, but the total current is half as much, making the resistance twice as great. Therefore, the resistance to ground of a vertical ground rod of depth  $L$  centimeters is

$$R = \frac{\rho}{2\pi L} \left( \log_e \frac{4L}{a} - 1 \right) \quad (13)$$

In general, if  $C$  includes the capacitance of the images of a conductor or conductors in the earth, the resistance to ground is

$$R = \frac{\rho}{2\pi C} \quad (14)$$

Vertical ground rods are widely used, sometimes in large groups, because they can be driven in place with little or no excavation and because they are likely to reach permanent moisture and earth of good conductivity.

#### TWO GROUND RODS IN PARALLEL

Let 2 ground rods of radius  $a$  centimeters be as shown in figure 2, and let them be electrically in parallel. Find the air capacitance  $C$  of the 2 rods and their images, that is, of 2 cylinders each of length  $2L$ . Let the cylinders have a uniform charge of  $q$  per centimeter. The potential at a point on one cylinder at a distance  $x$  from its center, caused by  $q \, dy$  on the other cylinder, is

$$\frac{q \, dy}{\sqrt{s^2 + y^2}}$$

The potential at  $x$  caused by the other cylinder is obtained by integrating this expression from  $y = 0$  to  $L - x$  and from  $y = 0$  to  $L + x$ . The average potential on one cylinder caused by uniform charge on the other is then obtained by multiplying by  $dx/L$  and integrating from  $x = 0$  to  $L$ , and is

$$\frac{2qL}{L} \log_e \frac{2L + \sqrt{s^2 + 4L^2}}{s} + \frac{s}{L} - \frac{\sqrt{s^2 + 4L^2}}{L} \quad (15)$$

For large values of  $s/L$ , this becomes

$$\frac{2qL}{s} \left( 1 - \frac{L^2}{3s^2} + \frac{2L^4}{5s^4} \dots \right) \quad (16)$$

For small values of  $s/L$ , it is

$$2q \left( \log_e \frac{4L}{s} - 1 + \frac{s}{2L} - \frac{s^2}{16L^2} + \frac{s^4}{512L^4} \dots \right) \quad (17)$$

Add the average potential of the cylinder caused by its own charge,

$$\frac{2qL}{C} = 2q \left( \log_e \frac{4L}{a} - 1 \right) \quad (18)$$

Divide by  $4qL$ , the total charge on the 2 cylinders, thus obtaining the value of  $1/C$  for the pair of ground rods and their images. Then, by equation 14, the resistance to ground of the pair of rods is

$$R = \frac{\rho}{4\pi L} \left( \log_e \frac{4L}{a} - 1 + \log_e \frac{2L + \sqrt{s^2 + 4L^2}}{s} + \frac{s}{2L} - \frac{\sqrt{s^2 + 4L^2}}{2L} \right) \quad (19)$$

or, for large values of  $s/L$ ,

$$R = \frac{\rho}{4\pi L} \left( \log_e \frac{4L}{a} - 1 \right) + \frac{\rho}{4\pi s} \left( 1 - \frac{L^2}{3s^2} + \frac{2L^4}{5s^4} \dots \right) \quad (20)$$

or, for small values of  $s/L$ ,

$$R = \frac{\rho}{4\pi L} \left( \log_e \frac{4L}{a} + \log_e \frac{4L}{s} - 2 + \frac{s}{2L} - \frac{s^2}{16L^2} + \frac{s^4}{512L^4} \dots \right) \quad (21)$$

A short alternative calculation for equation 20, which is found by trial to be good for spacings of 20 feet or more, is to replace each ground rod by a half-buried sphere which is equivalent in resistance

to one isolated ground rod. This procedure can be illustrated by a numerical example. The resistance to earth of a ground rod of  $3/4$ -inch diameter and 10-foot depth, by equation 13, is

$$R = \frac{\rho}{2\pi L} \times 6.155$$

The hemisphere which is buried and its image above the ground surface make a complete sphere whose air capacitance as an isolated conductor is, by a well known proposition, equal to its radius  $A$  in centimeters. By equation 14, the resistance to ground of the hemisphere is

$$R = \frac{\rho}{2\pi A}$$

Then the radius of the hemisphere which is equivalent to the isolated ground rod is, by equation 13,

$$A = \frac{L}{\log_e \frac{4L}{a} - 1} = \frac{L}{6.155}$$

Here,  $A$  and  $L$  may be both in centimeters or both in feet and so  $A = 10/6.155 = 1.625$  feet.

The capacitance of 2 equal spheres at a distance  $s$ , center to center, connected in parallel, is readily calculated when  $s$  is not small and the charges can be assumed uniformly distributed around the spheres. By symmetry, the spheres will carry equal charges. Let each charge be  $q$ . The potential of the surface of each sphere is

$$q \left( \frac{1}{A} + \frac{1}{s} \right)$$

and

$$\frac{1}{C} = \frac{1}{2} \left( \frac{1}{A} + \frac{1}{s} \right)$$

where the dimensions are in centimeters. Then

$$R = \frac{\rho}{4\pi} \left( \frac{1}{A} + \frac{1}{s} \right) \quad (20a)$$

This is the same as using the first term of the second part of equation 20.

From numerical examples, it is found that the results of equations 19 and 20a differ by about 0.5 per cent for 20-foot spacing between 2 ground rods, and by a few per cent for 10-foot spacing.

#### GROUPS OF GROUND RODS

The potential of a rod caused by its own charge and the charges of several other rods can be found by using equation 16 or 17 several times. Similarly, the potential of the surface of a sphere caused by its own charge and the charges of a number of other spheres is

$$\frac{q_1}{A} + \frac{q_2}{s_2} + \frac{q_3}{s_3} + \dots$$

where for an approximate calculation  $q_1, q_2, q_3$ , etc., may be assumed equal.

For somewhat better accuracy, the values of  $q$  for the rods near the center of the group may be taken a little lower than the values for the rods near the outer parts of the group, by an amount sufficient to make the potential of each rod the same. Thus the values for the outer parts may be taken equal to  $q$ , and others to  $0.95q$ ,  $0.9q$ , etc., according to judgment and to the test of equal potentials.

In order to design groups of ground rods for transmission line towers, stations and substation grounds, etc., and to decide on the best number and spacing of rods, it is desirable to be able to compare various groups of rods, assuming uniform conductivity of the soil. Accordingly, sets of curves are given in figures 3 to 6.<sup>2</sup> From them it is possible to estimate how many rods and how much area will be required for a certain number of ohms to ground in a given locality, from measurements on a few temporary test ground rods.

The basis of comparison is the resistance of one isolated ground rod of  $\frac{3}{4}$ -inch diameter and 10-foot depth. By means of figure 3, the resistance of single rods of various depths can be found and, if desired, the resistivity of the soil. In figure 4 the conductivity of 2, 3, and 4 rods is given in terms of the conductivity of isolated rods, and in figure 5 results are shown for larger numbers of rods.

In figure 6 the information is presented in different form, and the lowest resistance that can be obtained from a given area is shown. This information is often of value as it may be the means of preventing the wasteful

attempt of putting additional ground rods in an area which could not give the desired low resistance even if an infinite number of rods were used. For instance, if 36 ground rods are distributed as in figure 7 over a square area of 10,000 square

feet, that is, 100 by 100 feet, the spacing will be 20 feet. Figure 6 shows that the resistance is 1.3 times the resistance of an infinite number of rods in the same area. Therefore, no matter what the resistance in ohms may be or what the uniform conductivity of the ground may be, if it is desired to have less than 75 per cent of the resistance with 36 rods there is no use in putting more rods in the area of 10,000 square feet but it will be necessary to use a larger area.

Figure 6 shows also that if there are more than 10 rods 10 feet deep, there is no use in having closer than 10-foot spacing.

It is generally desirable not only to utilize the ground area effectively, but to make effective use of the rods, inasmuch as they represent a considerable cost. If one wishes the rods to be at least 60 per cent as effective as they would be if isolated, that is, to have at least 60 per cent of the conductivity of isolated rods, it may be seen from both figures 5 and 6 that it is necessary to use over 20-foot spacing for 16 rods in a square area, about 30-foot spacing for 25 rods, and over 40-foot spacing for 49 rods.

The curves of figures 5 and 6 are based on uniform distribution of ground rods in square areas, as shown in figure 7, the boundary of the area running through the outer rods. Although the curves are computed for square areas, they give an estimate for rectangular areas. The curves cannot be used for a part of a group of rods nor for a group which is near other groups, but a reading from the curves is to apply to

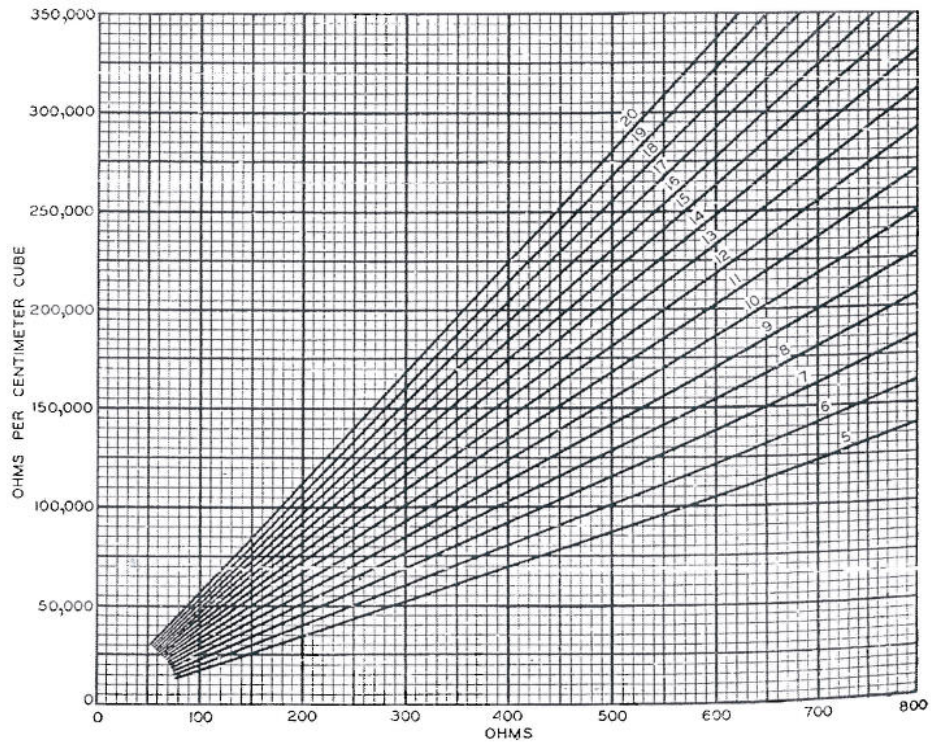


Fig. 3. Resistance of one ground rod of  $\frac{3}{4}$ -inch diameter

For low resistances divide both scales by 10; for high resistances multiply both scales by 10

Numbers on curves are depths in feet

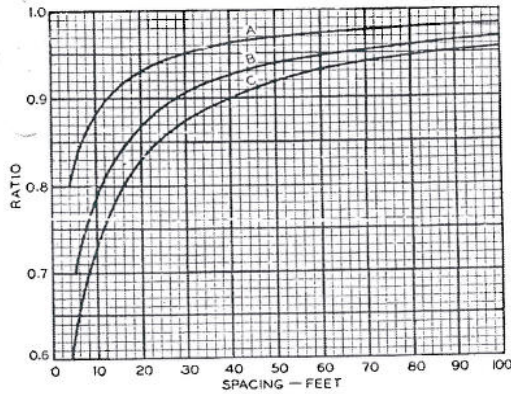


Fig. 4. Ratio of conductivity of ground rods in parallel to that of isolated rods

Ground rods are 3/4 inch in diameter, 10 feet deep; 3 rods on equilateral triangle, 4 rods on square  
 A—Two rods B—Three rods C—Four rods

area which contains all the ground rods in the vicinity.

In the calculation of cases involving more than 4 rods or the spheres which were substantially equivalent to them, equal charges were assumed for the spheres. The potential of a corner sphere was calculated and that of an innermost sphere and the average taken, thus approximating the Howe average potential method. For a small number of spheres this was checked and good agreement obtained by computing the actual charges by simultaneous equations. For a large number of ground rods, the results shown in figures 5 and 6 are approximate.

The effect of the buried wires used to connect the ground rods together was not included in the computations for the figures which have been described. If the conductivity of each ground rod be assumed to be increased by the same percentage by the connecting wires, the latter will have little effect on the comparison of different groups of rods made by means of the curves.

#### BURIED HORIZONTAL WIRE

In some cases, connection to the earth is made by means of a buried horizontal wire. The image of this wire in the ground surface requires the use of equation 19 or 21 where, in this case, the length of the buried wire is  $2L$  centimeters and the distance from the wire to its image is  $s$  centimeters, which is twice the distance from the wire to the ground surface. If the image were not taken into account, a serious change in the result would often ensue.

*Example.* Length of No. 4/0 wire, 200 feet; depth, 10 feet;  $\rho$ , 200,000 ohms per centimeter cube.  $R = 57.6$  ohms

#### TWO PARALLEL BURIED WIRES

The resistance to ground of 2 parallel buried wires, including the effect of their images in the ground

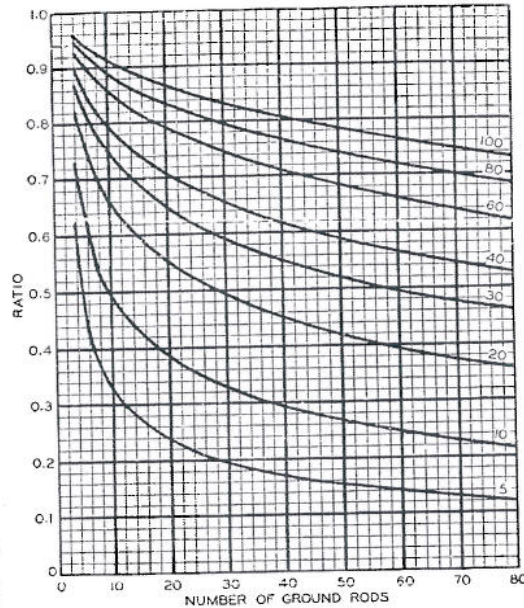


Fig. 5. Ratio of conductivity of ground rods in parallel on an area to that of isolated rods

Numbers on curves are spacings in feet

surface, is calculated by the same method as for 4 ground rods at the corners of a rectangle. The average potential of one of the wires caused by its own charge, equation 18, is to be added to the average potential caused by each of the other wires. Thus, one item is to be computed by equation 18 and 3 items by equation 15 or 17, using 3 values of  $s$ . The sum, divided by the total charge of the 4 wires,  $8qL$ , is  $1/C$  and then equation 14 can be applied.

*Example.* To find: the resistance to ground of 2 wires, 100 feet long, 0.46 inch in diameter, 7 feet apart, and 10 feet below the surface of the ground, the resistivity of the ground being 200,000 ohms per centimeter cube. The wires are connected in parallel, electrically.

Potential of a wire caused by its own charge, by equation 18	16.51 $q$
Potential by equation 15 or 17 for $s = 7$	4.84 $q$
Potential by equation 15 or 17 for $s_1 = 20$	2.99 $q$
Potential by equation 15 or 17 for $s_2 = 21.19$	2.89 $q$
Potential	27.23 $q$

Total charge =  $4 \times 1200 \times 2.540 \times q = 12,190 q$

$$\frac{1}{C} = \frac{27.23}{12,190}$$

$$R = \frac{\rho}{2\pi C} = \frac{200,000 \times 27.23}{2\pi \times 12,190} = 71.1 \text{ ohms}$$

#### RIGHT-ANGLE TURN OF WIRE

If the buried wire forms a right angle each arm of which is  $L$  centimeters in length the depth below

The ground surface being  $s/2$ , the resistance to ground including the effect of the image wires is

$$R = \frac{\rho}{4\pi L} \left( \log_e \frac{2L}{a} + \log_e \frac{2L}{s} - 0.2373 + 0.2146 \frac{s}{L} + 0.1035 \frac{s^2}{L^2} - 0.0424 \frac{s^4}{L^4} \dots \right) \quad (22)$$

where  $a$  is the radius of the wire.

*Example.* Length of each arm of No. 4/0 wire, 100 feet; depth, 10 feet;  $\rho$ , 200,000 ohms per centimeter cube.  $R = 59.4$  ohms

### THREE-POINT STAR

If there are 3 buried wires of length  $L$  which meet each other at 120 degrees, the resistance to ground including the effect of images is

$$R = \frac{\rho}{6\pi L} \left( \log_e \frac{2L}{a} + \log_e \frac{2L}{s} + 1.071 - 0.209 \frac{s}{L} + 0.238 \frac{s^2}{L^2} - 0.054 \frac{s^4}{L^4} \dots \right) \quad (23)$$

*Example.* Length of each arm of No. 4/0 wire, 100 feet; depth, 10 feet;  $\rho$ , 200,000 ohms per centimeter cube.  $R = 43.9$  ohms

### FOUR-POINT STAR

$$R = \frac{\rho}{8\pi L} \left( \log_e \frac{2L}{a} + \log_e \frac{2L}{s} + 2.912 - 1.071 \frac{s}{L} + 0.645 \frac{s^2}{L^2} - 0.145 \frac{s^4}{L^4} \dots \right) \quad (24)$$

*Example.* Same values of dimensions as for 3-point star.  $R = 37.3$  ohms

### SIX-POINT STAR

$$R = \frac{\rho}{12\pi L} \left( \log_e \frac{2L}{a} + \log_e \frac{2L}{s} + 6.851 - 3.128 \frac{s}{L} + 1.758 \frac{s^2}{L^2} - 0.400 \frac{s^4}{L^4} \dots \right) \quad (25)$$

*Example.* Same values of dimensions as for 3-point star.  $R = 31.1$  ohms

### EIGHT-POINT STAR

$$R = \frac{\rho}{16\pi L} \left( \log_e \frac{2L}{a} + \log_e \frac{2L}{s} + 10.98 - 5.51 \frac{s}{L} + 3.20 \frac{s^2}{L^2} - 1.17 \frac{s^4}{L^4} \dots \right) \quad (26)$$

*Example.* Same values of dimensions as for 3-point star.  $R = 28.2$  ohms

Equations 22 to 26, being simple power series, save considerable time in computing numerical results.

If  $L$  is in centimeters and  $\rho$  in ohms per centimeter cube,  $R$  is in ohms. Also, if  $L$  is in inches and  $\rho$  in ohms per inch cube,  $R$  is in ohms. Inside the brackets, only ratios of dimensions occur. The numerator of each fraction must be in the same units as the denominator of that fraction. Note that  $s$  is the distance from the wire to the image, and is twice the distance from the wire to the ground surface.

In order to estimate relative accuracy, the potential of the wire at various distances from the center of a 4-point star was plotted and compared with the potential distribution of a round plate. The poten-

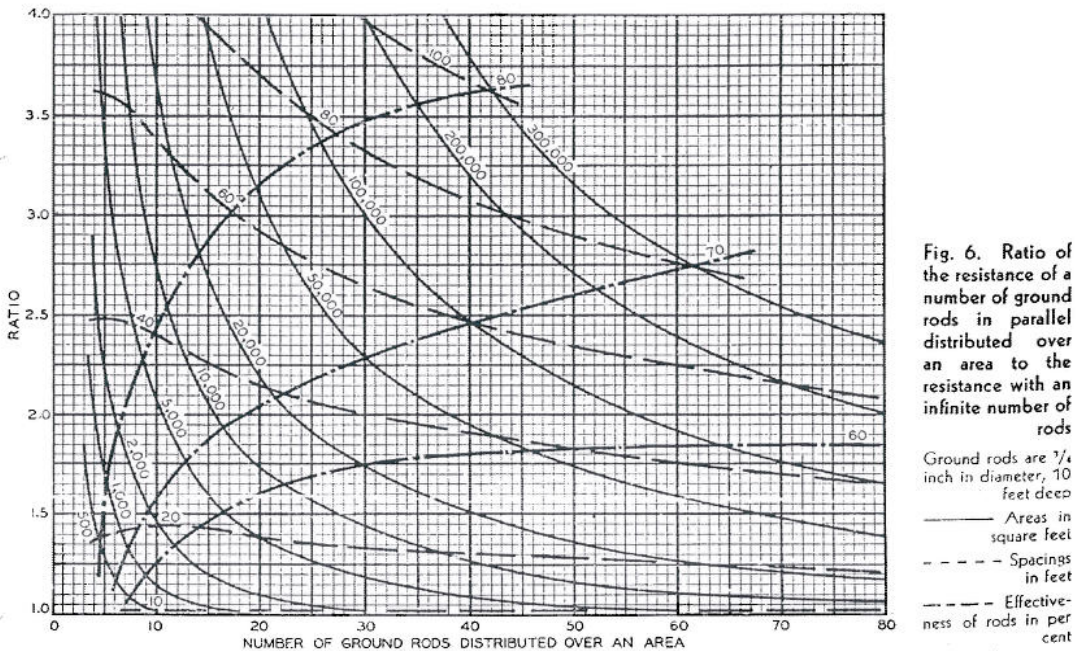








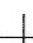

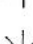




Fig. 6. Ratio of the resistance of a number of ground rods in parallel distributed over an area to the resistance with an infinite number of rods  
Ground rods are 1/4 inch in diameter, 10 feet deep  
—— Areas in square feet  
- - - - Spacings in feet  
- · - · Effectiveness of rods in per cent

tial distribution in the 2 cases showed approximately the same amount of deviation from the average potential. Accordingly, it can be concluded that the resistance of stars of wire obtained by

on another equal wire which meets it at one end at angle  $\theta$  is given by the simplified expression

$$V_{av} = 2q \log_e [1 + \operatorname{cosec} (\theta/2)] \quad (27)$$

Table I—Approximate Formulas Including Effect of Images

	One Ground Rod Length $L$ , radius $a$	$R = \frac{\rho}{2\pi L} \left( \log_e \frac{4L}{a} - 1 \right)$	(13)
	Two Ground Rods $s > L$	$R = \frac{\rho}{4\pi L} \left( \log_e \frac{4L}{a} - 1 \right) + \frac{\rho}{4\pi s} \left( 1 - \frac{L^2}{3s^2} + \frac{2}{5} \frac{L^4}{s^4} \dots \right)$	(20)
	Two Ground Rods $s < L$	$R = \frac{\rho}{4\pi L} \left( \log_e \frac{4L}{a} + \log_e \frac{4L}{s} - 2 + \frac{s}{2L} - \frac{s^2}{16L^2} + \frac{s^4}{512L^4} \dots \right)$	(21)
	Buried Horizontal Wire Length $2L$ , depth $s/2$	$R = \frac{\rho}{4\pi L} \left( \log_e \frac{4L}{a} + \log_e \frac{4L}{s} - 2 + \frac{s}{2L} - \frac{s^2}{16L^2} + \frac{s^4}{512L^4} \dots \right)$	(21)
	Right-Angle Turn of Wire Length of arm $L$ , depth $s/2$	$R = \frac{\rho}{4\pi L} \left( \log_e \frac{2L}{a} + \log_e \frac{2L}{s} - 0.2373 + 0.2146 \frac{s}{L} + 0.1035 \frac{s^2}{L^2} - 0.0424 \frac{s^4}{L^4} \dots \right)$	(22)
	Three-Point Star Length of arm $L$ , depth $s/2$	$R = \frac{\rho}{6\pi L} \left( \log_e \frac{2L}{a} + \log_e \frac{2L}{s} + 1.071 - 0.209 \frac{s}{L} + 0.238 \frac{s^2}{L^2} - 0.054 \frac{s^4}{L^4} \dots \right)$	(23)
	Four-Point Star Length of arm $L$ , depth $s/2$	$R = \frac{\rho}{8\pi L} \left( \log_e \frac{2L}{a} + \log_e \frac{2L}{s} + 2.912 - 1.071 \frac{s}{L} + 0.645 \frac{s^2}{L^2} - 0.145 \frac{s^4}{L^4} \dots \right)$	(24)
	Six-Point Star Length of arm $L$ , depth $s/2$	$R = \frac{\rho}{12\pi L} \left( \log_e \frac{2L}{a} + \log_e \frac{2L}{s} + 5.851 - 3.125 \frac{s}{L} + 1.758 \frac{s^2}{L^2} - 0.490 \frac{s^4}{L^4} \dots \right)$	(25)
	Eight-Point Star Length of arm $L$ , depth $s/2$	$R = \frac{\rho}{16\pi L} \left( \log_e \frac{2L}{a} + \log_e \frac{2L}{s} + 10.98 - 5.51 \frac{s}{L} + 3.26 \frac{s^2}{L^2} - 1.17 \frac{s^4}{L^4} \dots \right)$	(26)
	Ring of Wire Diameter of ring $D$ , diameter of wire $d$ , depth $s/2$	$R = \frac{\rho}{2\pi^2 D} \left( \log_e \frac{8D}{d} + \log_e \frac{4D}{s} \right)$	(29)
	Buried Horizontal Strip Length $2L$ , section $a$ by $b$ , depth $s/2$ , $b < a/8$	$R = \frac{\rho}{4\pi L} \left( \log_e \frac{4L}{a} + \frac{c^2 - \pi ab}{2(a+b)^2} + \log_e \frac{4L}{s} - 1 + \frac{s}{2L} - \frac{s^2}{16L^2} + \frac{s^4}{512L^4} \dots \right)$	(31)
	Buried Horizontal Round Plate Radius $a$ , depth $s/2$	$R = \frac{\rho}{8a} + \frac{\rho}{4\pi s} \left( 1 - \frac{7}{12} \frac{a^2}{s^2} + \frac{33}{40} \frac{a^4}{s^4} \dots \right)$	(32), (36)
	Buried Vertical Round Plate Radius $a$ , depth $s/2$	$R = \frac{\rho}{8a} + \frac{\rho}{4\pi s} \left( 1 + \frac{7}{24} \frac{a^2}{s^2} + \frac{99}{320} \frac{a^4}{s^4} \dots \right)$	(32), (38)

equations 23 to 26 is an approximation within several per cent.

In deriving the formulas for stars of wire, the average potential on one branch caused by its own charge is computed and added to that caused by each of the other branches and the images. The total potential, divided by the total charge of all the branches and their images, gives  $1/C$  and then equation 14 is used.

For these computations, the formulas in appendix 2 of reference 3 are used. In this connection, the average potential of one wire caused by the charge

If  $\theta$  should be extremely small, the radius of the wire would need to be brought into the computation, and equation 27 would be inapplicable.

#### BURIED RING OF WIRE

The capacitance of an isolated ring of round wire is given by

$$\frac{1}{C} = \frac{2}{\pi D} \log_e \frac{8D}{d} \quad (28)$$

where the diameter of the ring,  $D$  centimeters, is



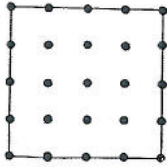


Fig. 7. Distribution of ground rods used for calculating the curves

much larger than the diameter of the wire,  $d$  centimeters. The resistance to ground of a deeply buried ring is then  $R = \rho/4\pi C$  as in equation 11.

The capacitance of a ring and its image at distance  $s$  is given by

$$\frac{1}{C} = \frac{1}{\pi D} \left( \log_e \frac{8D}{d} + \log_e \frac{4D}{s} \right) \quad (29)$$

where  $s$  is considerably larger than  $d$  and also considerably smaller than  $D$ .<sup>12</sup> The resistance to ground of a buried horizontal ring, taking the effect of the ground surface into account, is then  $R = \rho/2\pi C$  as in equation 14. Note that  $s$  is twice the distance from the ring to the ground surface.

#### BURIED STRIP CONDUCTOR

The capacitance of an isolated strip conductor, whose length  $2L$  centimeters is large compared with its width  $a$  centimeters or its thickness  $b$  centimeters, is given by

$$\frac{1}{C} = \frac{1}{L} \left( \log_e \frac{4L}{a} + \frac{a^2 - \pi ab}{2(a+b)^2} \right) \quad (30)$$

For a description of the derivation, see equation 27 of reference 2. The thickness  $b$  should be less than about  $1/8$  of the width  $a$ .

In most cases, the effect of the image should be included, as follows:

$$\frac{1}{C} = \frac{1}{2L} \left( \log_e \frac{4L}{a} + \frac{a^2 - \pi ab}{2(a+b)^2} + \log_e \frac{4L}{s} - 1 + \frac{s}{2L} - \frac{s^2}{16L^2} + \frac{s^4}{512L^4} \dots \right) \quad (31)$$

where  $s$  is the distance in centimeters from the strip to the image, that is, twice the distance to the ground surface. The resistance to ground, when equation 31 is used, is  $R = \rho/2\pi C$  as in equation 14.

#### ROUND PLATE

The capacitance of a single isolated thin round plate is given by<sup>13</sup>

$$\frac{1}{C} = \frac{\pi}{2a} = \frac{1.571}{a} \quad (32)$$

where  $a$  is the radius of the plate in centimeters.

It is of interest to show that the average potential method, if used in this case, produces an error of 8 per cent, giving a value of  $1/C$  which is 8 per cent too large. Expressions for the potential caused by a ring carrying uniform charge density are given in reference 10, pages 11 and 153. From these is obtained the average potential of a thin round plate of radius  $a$  centimeters caused by a uniform charge

density  $q$  per square centimeter in the form of 3 series whose sum is

$$V_{av} = \frac{2\pi qa}{3} \left( 2 + \frac{1}{4} + \frac{3^2}{4^2 \times 6} + \frac{3^2 \times 5^2}{4^2 \times 6^2 \times 8} + \dots \right) \quad (33)$$

The sum of this slowly converging series can be found by comparing it with the series

$$\frac{\pi^2}{8} = 1 + \frac{1}{3^2} + \frac{1}{5^2} + \frac{1}{7^2} + \dots \quad (34)$$

Multiply the terms within the brackets of equation 33 by 0.401723 to make the eleventh terms of equations 33 and 34 alike. It is found that  $1/C$  or  $V_{av}/\pi a^2 q$  is slightly greater than  $1.69721/a$ . Multiply the terms within the bracket of equation 33 by 0.329595 to make its tenth term equal to the eleventh term of equation 34 and all its succeeding terms distinctly less than the corresponding terms of equation

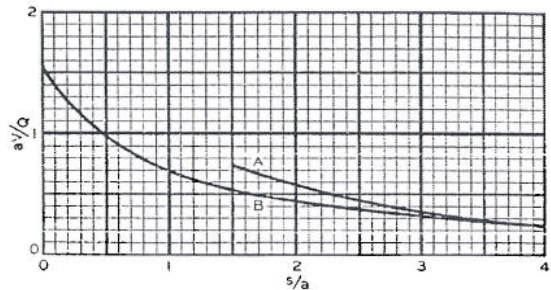


Fig. 8. Average potential on a round plate caused by an equal plate

A Some plane B Parallel planes  
 $a$  — radius of plates in centimeters

34. It is found that  $1/C$  is less than 1.70169/a. The difference between the 2 limiting values is 0.27 per cent and an inspection of the series shows that the value of  $1/C$  by the average potential method is much nearer the smaller limit than the larger, and so is nearly equal to

$$\frac{1.6972}{a} \quad (35)$$

The true value of  $1/C$  is, however, by equation 32,

$$\frac{\pi}{2a} = \frac{1.5708}{a}$$

The average potential method, therefore, gives a value of  $1/C$  for a thin round plate which is 8 per cent too high.

This result has been confirmed by Dr. F. W. Grover by a method using mechanical integration, which gave

$$\frac{V_{av}}{\pi a^2 q} = \frac{1.6966}{a}$$

There is a connection between the error caused by the average potential method and the amount of the

variation in potential over the conductor caused by uniform charge distribution. The potential of the center of the plate resulting from uniform charge distribution is  $2\pi a q$ , using the formulas of reference 10. However, the average value is

$$\frac{.97}{a} \times \pi a^2 q = 1.697\pi a q$$

Thus, the potential of the center is seen to be 18 per cent higher than the average potential. This comparatively large percentage may account in some degree for the 8 per cent error in the case of a round plate, resulting from the use of the average potential method. In the case of the cylinder of the length considered in this paper, the potential of the middle point was 4.7 per cent higher than the average potential (see reference 2) and in that case the average potential method was shown to give a very nearly correct value of  $1/C$ .

#### TWO ROUND PLATES IN PARALLEL PLANES

The potential caused by a charged round plate, at points not near the plate, is given by the last series on page 154 of reference 10. Integrating that series over the surface of a second disk having the same axis and the same length of radius as the first, the average potential on the second disk caused by the charge on the first is

$$V_{av} = \frac{Q}{s} \left( 1 - \frac{7}{12} \frac{a^2}{s^2} + \frac{33}{40} \frac{a^4}{s^4} \dots \right) \quad (36)$$

where  $Q$  is the total charge in statfarads on the first disk,  $a$  is the radius in centimeters of both plates, and  $s$  is the distance in centimeters between the 2 plates.

This power series should not be used unless the last term is quite small and so the largest value of  $a/s$  for which it is useful is about  $1/2$ . Since equation 36 gives the average potential, it is not a precise calculation for capacitance or resistance. However, the order of its precision may be estimated by finding the potential at the center of the second disk, which is  $(Q/s) \tan^{-1}(a/s)$  (see the series on page 154 of reference 10).

Where  $s = 2a$ , the potential at the center is 4 per cent greater than the average potential, and for larger values of the separation  $s$  the discrepancy is smaller. It may be remembered that for one isolated round plate the potential of the center was 18 per cent more than the average potential, and the error in the value of capacitance was 8 per cent. In the case of the calculation for one isolated ground rod of average proportions the potential at the middle of the cylinder is 4.7 per cent greater than the average potential, and the error in the capacitance is less than 1 per cent.<sup>2</sup> It may be concluded that the use of average potential gives the same order of accuracy in the case of equation 36 as in the case of a long cylinder.

Values of  $aV/Q$  calculated by equation 36 are plotted in figure 8. This curve has been extended to apply to small values of  $s$  by taking the average values obtained by using the 2 series on page 154, reference 10, to compute the potential at the rim and at the center of the second disk caused by the charge on the first disk. This process is shown to give good results by comparing it with equation 36 for  $s/a$  between 2 and 4. The potential at the rim is equal to the potential at the center when  $s = 0$ . More accurate values for the curve of figure 8 could be computed by dividing the circular area into

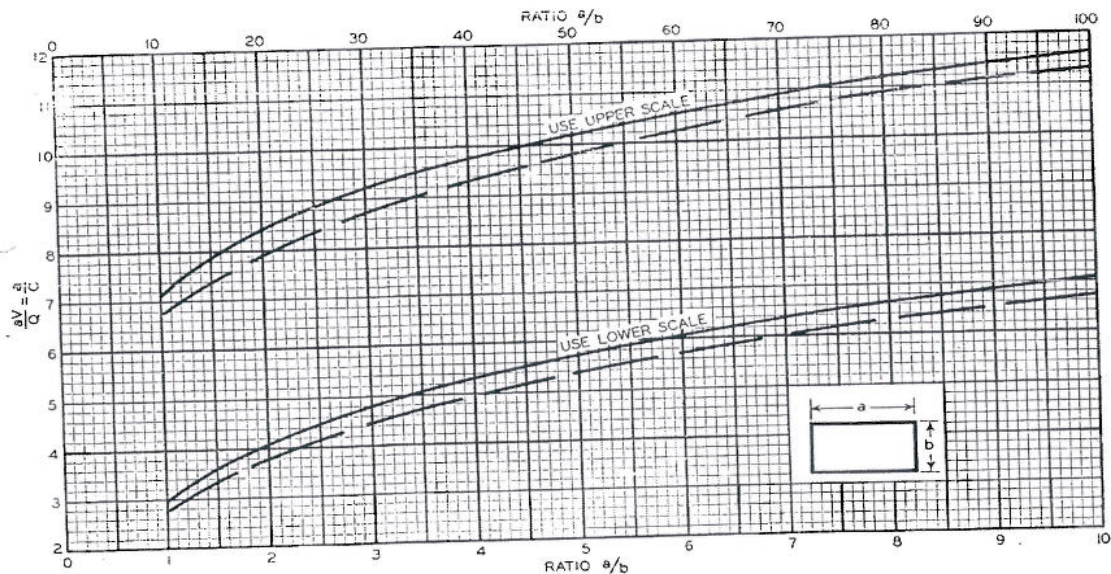


Fig. 9. Capacitance of a rectangular plate  
Dimension  $a$  in centimeters;  $C$  in statfarads

bands, computing the potential for each band, and averaging, this being a process of mechanical integration. However, no matter how carefully this might be done, the result would be subject to the error inherent in the average potential method.

It may be seen from equation 36 that when the separation is large, the potential on one plate caused by the other is given closely by

$$V = \frac{Q}{s} \quad (37)$$

which is the same as assuming that the charge is on the surface of a sphere, or concentrated at a point. For example, when  $s/a = 5$ , the result of equation 37 is 2 per cent larger than that of equation 36 and the value of  $Q/s$  itself is only 13 per cent of the potential of an isolated plate to which it is to be added. Accordingly, equation 37 can usually be used for the images of the buried plates, which are at distances  $s_1$  and  $s_2$ , center to center.

Where the 2 round plates are connected in parallel, then in the capacitance problem the plates and their images all carry charges equal to  $Q$ . By symmetry, the potential is the same for them all, and is made up of the following 4 items which are added together. First, the potential,  $\pi Q/(2a)$ , given by equation 32, caused by the plate's own charge; second, the potential given by equation 36, caused by the other coaxial buried plate which lies in a vertical plane parallel to that of the first plate; third, the potential  $Q/s_1$ , caused by the plate's image, where  $s_1$  is the distance in centimeters from the center of the plate to the center of the image, that is,  $s_1$  is twice the distance to the surface of the ground; fourth, the potential  $Q/s_2$ , caused by the other image.

The sum of these 4 items is equal to  $V$  and the capacitance of the 4 plates is given by  $1/C = V/(4Q)$ . Then the resistance to ground of the 2 buried plates connected in parallel is  $R = \rho/(2\pi C)$  by equation 14.

Where the 2 round plates are connected in series, in the resistance problem current flows from one to the other through the ground and in the capacitance problem one plate carries a charge  $Q$  and the other  $-Q$ . The images carry charges  $Q$  and  $-Q$ , each being of the same sign as the charge directly beneath it. Equations 11 and 14 are still used to change from the capacitance problem to the resistance problem.

#### TWO ROUND PLATES IN THE SAME PLANE

Where the 2 plates of radius  $a$  in centimeters are in the same plane, the average potential on one resulting from the charge on the other is

$$V_{av} = \frac{Q}{s} \left( 1 + \frac{7}{24} \frac{a^2}{s^2} + \frac{99}{320} \frac{a^4}{s^4} + \dots \right) \quad (38)$$

In this case, there is more error in the use of average potential than in equation 36, for when  $s/a = 2$ , the potential at the center differs from the average potential by 19 per cent. As in other cases, if the term in  $a^2/s^2$  is negligibly small compared to 1, the simple expression  $Q/s$  may be used

and the error resulting from the use of average potential is negligible.

#### RECTANGULAR PLATES

The capacitance of an isolated thin rectangular plate,  $a$  centimeters by  $b$  centimeters, according to the average potential method, is given by<sup>9</sup>

$$\frac{1}{C} = 2 \left( \frac{1}{a} \log_e \frac{a + \sqrt{a^2 + b^2}}{b} + \frac{1}{b} \log_e \frac{b + \sqrt{a^2 + b^2}}{a} + \frac{a}{3b^2} + \frac{b}{3a^2} - \frac{(a^2 + b^2)\sqrt{a^2 + b^2}}{3a^2b^2} \right) \quad (39)$$

The potential of the center of a square plate is 18 per cent greater than the average potential, and this difference is 15 per cent for a rectangle whose length is 5 times its width. Accordingly, the correction for the average potential method found for a circular plate will apply, and 8 per cent should be subtracted from the value of  $1/C$  given by equation 39 for a square or nearly square plate, and almost as much should be subtracted for a rectangular plate of length about 5 times the width. The full lines of figure 9 show values calculated by equation 39 and the broken lines show estimated corrected values (see the paragraphs following equation 32 of reference 2).

A formula for the average potential of a rectangular plate caused by a uniformly distributed charge on a similar plate in the same plane can be given but it is not short and it is subject to the errors inherent in the average potential method. It seems better to replace the rectangular plates by circular plates of the same area and on the same centers, and to use equation 36, 37, or 38 for the effect of one plate on another.

#### REFERENCES

1. LÖSUNG ZWEIER POTENTIALPROBLEME DER ELEKTROSTATIK, E. HALLG, *Arkiv för Matematik, Astronomi och Fysik*, v. 21A, No. 22, 1929 Stockholm.
2. CALCULATION OF RESISTANCES TO GROUND AND OF CAPACITANCE, H. B. DWIGHT, *Journal of Mathematics and Physics*, v. 10, 1931, No. 1, p. 50.
3. METHODS, FORMULAS AND TABLES FOR THE CALCULATION OF ANTENNA CAPACITY, F. W. GROVER, Scientific Paper No. 568 of the Bureau of Standards, Washington, D. C., 1928, page 569.
4. CAPACITY OF RADIO-TELEGRAPH ANTENNAS, G. W. O. HOWE, *The Electrician*, v. 73, 1914, p. 829, 859, and 906.
5. CAPACITY OF AERIALS OF THE UMBRELLA TYPE, G. W. O. HOWE, *The Electrician*, v. 75, 1915, p. 870.
6. CALCULATION OF THE EFFECTIVE RESISTANCE OF EARTH PLATES, G. W. O. HOWE, *The Electrician*, v. 76, 1915, p. 353.
7. CALCULATION OF THE CAPACITY OF RADIO-TELEGRAPH ANTENNAS INCLUDING THE EFFECT OF MASTS AND BUILDINGS, G. W. O. HOWE, *The Electrician*, v. 77, 1916, p. 761 and 880.
8. CAPACITY OF AN INVERTED CONE AND THE DISTRIBUTION OF ITS CHARGE, G. W. O. HOWE, *Physical Society of London Journal*, v. 29, 1917, p. 339.
9. CAPACITY OF RECTANGULAR PLATES AND A FORMULA FOR CAPACITY OF AERIALS, G. W. O. HOWE, *Radio Review*, Nov. 1920, p. 710.
10. FOURIER'S SERIES AND SPHERICAL, CYLINDRICAL, AND HELIPODAL HARMONICS (a book), W. E. BYERLY, Ginn and Company, Boston, Mass., 1893.
11. GROUND CONNECTIONS FOR ELECTRICAL SYSTEMS, Technologic Paper No. 108 of the Bureau of Standards, Washington, D. C.
12. DIE AUSBREITUNG DER LUFT- UND ERDFELDER UM HOCHSPANNUNGSLEITUNGEN BESONDERS DREI ERD- UND KURZSCHLÜSSEN, R. RÜDENBERG, *Elektrotechnische Zeitschrift*, v. 46, Sept. 3, 1925, p. 1342.
13. THE NEWTONIAN POTENTIAL FUNCTION (a book), B. O. PEIRCE, Ginn & Co., Boston, Mass., 1902, p. 161.
14. ERDSTRÖME (a book), F. OLTENDORFF, Julius Springer, Berlin, 1928.

## Measurements and Computations of the Performance of Grounding Systems Buried in Multilayer Soils

F. Dawalibi, Senior Member  
Safe Engineering Services & technologies Ltd.  
1544 Viel, Montreal, Canada, H3M-1G4

N. Barbeito, Member  
Florida Power Corporation  
St. Petersburg, Florida 33733

### ABSTRACT

The resistances and earth surface potentials of two Florida Power Corporation electric substation grounding systems buried in soils with multiple horizontal layers were computed and measured at various phases of their installation. i.e., starting from a one mesh grid to the final design consisting of many regular meshes. Soil resistivity at each site was measured and interpreted to obtain equivalent two-layer and multilayer earth structures. It is shown that good agreement is obtained between the measured and computed values if multilayer earth structure models are used in the computations. Poor agreements are achieved when uniform soil models are considered.

*KEYWORDS: Measurements, Computer Modelling, Multilayer Soils, Grounding, Touch Potentials.*

### 1.0 INTRODUCTION

Computerized grounding analysis in uniform and two-layer soil types became widespread in the eighties, mainly because of the enhanced accuracy, speed and flexibility afforded by the use of modern computers. Several publications [1-5] have discussed the analytical methods used when uniform and two-layer soils are involved. Other publications [7,8] have examined in detail computerized results of ground system performance in uniform and two-layer soils. There are a few papers which compare analytical results with measured ones obtained in scaled-down two-layer models [8,9] and in the field where the earth structure can be approximated by uniform or two-layer models [10,11].

Although the first author has been modelling grounding systems in multilayer soils for several years at his company and has often been involved in studies conducted by other power utility engineers<sup>1</sup>, he is not aware of any publications available in the open literature which discuss and compare computer-generated results with field measurements involving multilayer soils. The field tests presented in this paper are of particular interest because they were performed on substation

91 WM 037-2 PWRD A paper recommended and approved by the IEEE Substations Committee of the IEEE Power Engineering Society for presentation at the IEEE/PES 1991 Winter Meeting, New York, New York, February 3-7, 1991. Manuscript submitted August 29, 1990; made available for printing January 3, 1991.

grids which were tested at different stages of construction. Ground potential rise (GPR) and touch voltages are of particular interest. This paper fills this gap in the literature, at least for horizontally layered soils, and illustrates the case of vertical stratification using the example of a simple ground grid buried in a soil with three arbitrary vertical layers.

### 2.0 ANALYTICAL CONSIDERATIONS

Analysis of grounding systems in nonuniform earth has been discussed in sufficient detail for two-layer soils [1-11] (see also IEEE Guide #80 [12] for an extensive list of references). There have been only a few publications dealing with the subject of soils with more than two layers [13,14]. The methods described in these publications however, have been developed for HVDC toroidal electrodes and have used a brute-force approach based on the method of optical images where a sufficient number of images are computed in order to achieve the desired accuracy. These methods appear practical only on supercomputers capable of performing several hundreds of megaflops per second. On slower computers, the methods which are normally used to reduce computation time fall into 3 categories:

- 1- Those based on the method of images, where the depths of the layer interfaces are a multiple of a base layer.
- 2- Those based on convolution and linear filter theories.
- 3- Those based on direct numerical integration.

The first method was introduced by Stefanescu and Schlumberger in 1930 [15]. It has since been refined by geophysicists (see for example, Mooney and Orellana [16] and Flathe [17]) and has been used extensively in resistivity analysis problems. It was adapted to power system problems by Dawalibi [10,18] in the early eighties. Although there has been a recent publication dealing with the subject of soil resistivity in multilayer earth (see Takahashi and Kawase [19] and the discussion at the end of their paper), the theory underlying the basic principles is well known and will not be discussed here despite the fact that the power system engineering community is usually unfamiliar with this work. It is believed that the open literature (see for example Keller [20]) contains detailed information for the reader interested in this subject. Once those techniques are mastered, it is a relatively easy task to proceed

<sup>1</sup> These studies have been conducted since 1986 by North-American utilities using the MALT software code referenced in IEEE Guide #80 [12].

from the point source analytical expressions to those involving straight ground conductor segments. The methodology is the same as that used for two-layer soils, except that one has to account for multiple infinite series of images of the conductor segment at each location whereas only one infinite series of images is expected for two-layer soils. The technique follows that developed by Oslon et al [21]. We are also aware of an unpublished paper by Delici et al which used this technique. The numerical results presented in this paper for the case of multiple horizontal layers are based on this technique of subdividing the soil into layers with thicknesses equal to a multiple of a base value.

The second method is based on more recent work introduced by Ghosh [22] in the early seventies. It is extensively used for interpreting soil resistivity measurements in multilayer soils. This is the method used in this paper to examine soil resistivity measurements at the two FPC substations. Research work is presently in progress at SES to implement this fast and powerful "point source" method to the case of conductor segments buried in multilayer soils.

The third method is the subject of a companion paper [23] and will not be discussed here. It is worthwhile to note that this method has the potential of dealing with multilayer soils and curvilinear conductors at the same time. It does require, however, more elaborate analytical expressions and more computation time than the preceding methods.

### 3.0 FIELD MEASUREMENTS

Earth resistivity measurements were conducted before and after the installation of the grounding systems at FPC Bayridge and West Davenport Substations. The grounding systems were later installed in progressive steps starting first with the outermost loop and then adding conductors until the final design consisting of small square meshes was completed. Both the GPR and mesh voltages were measured at the end of each construction step. The measurements were not carried out initially with the knowledge that later, computer model results were to be compared with the field values. For that reason, the position of earth surface potential measurement observation points and the exact location of the ground conductors as installed by the contractor were not determined with great accuracy. It is estimated that the error on those positions is on the order of 10 to 15%. The measured and computed results are described hereafter.

Field tests were performed on substation ground grids isolated from the power system neutral paths. Resistivity tests were performed using the Wenner configuration. Resistance tests were performed based on the Fall-of-Potential technique. The grids were energized at 120 V ac with a portable generator and with the return current probe installed 1,000 feet away from the grid. Mesh voltages consisted in the measured difference between the ground grid GPR and the local soil potentials.

### 3.1 BAYRIDGE SUBSTATION

Figure 3.1 shows the initial, intermediate and ultimate shapes of this non rectangular substation grounding grid. The final

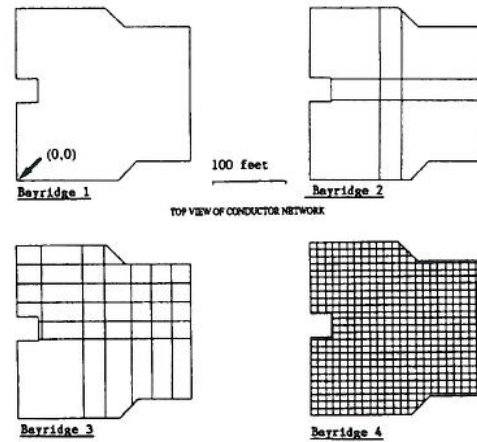


Figure 3.1 Bayridge Substation Grid During Various Stages of its Construction

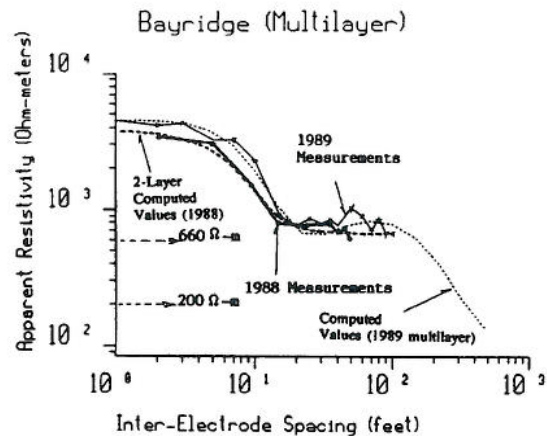


Figure 3.2 Measured and Computed Soil Resistivity at Bayridge Substation

grid consists of about 450 regular square meshes (about  $10' \times 10'$ ) [24]. The origin of the coordinate system used in the computer modelling is the lower left hand corner. The origin of the first 3-D profile in Figures 3.3 and 3.4 is at (-50,-50).

Resistivity measurements were carried out inside and outside the substation area, before and after grid construction respectively (in 1988, then in 1989). The field results are shown in Figure 3.2. This figure also shows computation results based on a two-layer soil structure and a six-layer structure, as defined in the first part of Table 3.1. Two other variations of these soil models were examined also. They will not be discussed in this paper.

The two-layer earth structure model was determined from the 1988 resistivity measurements which exhibited an anomalous reading at the 100 foot spacing. This reading was discarded during the interpretation of the field resistivity results. The

six-layer model is based on the most recent measurements which were conducted in order to resolve the uncertainty in the apparent resistivity at spacings larger than 50 feet. The measurement traverse however was located outside the substation area. The new information from the multilayer soil model suggested the lower bottom soil resistivity of the alternative two-layer soil model.

The substation GPR and mesh (touch) voltages were computed based on both earth structure models for each one of the four grid configurations tested during the construction stages. Table 3.2 summarizes the salient results obtained from the measurements and computations. Figures 3.3 and 3.4 are 3-D views of the earth surface touch voltages which exist above and in the vicinity of the substation grid for Stages 1 and 3 of the construction. These plots are based on the six-layer earth structure model.

MODEL TYPE	LAYER NO.	LOCATION	LAYER THICKNESS (Feet)	LAYER RESISTIVITY (Ohm-m)
2 Layers	1	Top	4.46	3728.0
	2	Bottom	-	660.0
6 Layers	1	Top	6.10	4520.0
	2	Central	9.2	278.0
	3	Central	10.4	764.0
	4	Central	39.2	1491.0
	5	Central	32.8	818.5
	6	Bottom	-	100.0
2 Layers Alternative	1	Top	6.57	3380.0
	2	Bottom	-	200.0

Table 3.1 Best Fit Soil Structure Models at Bayridge Substation

GRID SHAPE	TWO-LAYER MODEL	ALTERNATIVE 2-LAYER MODEL	MULTILAYER MODEL	MEASURED VALUES
BAYRIDGE 1	16.60	13.95	18.35	14.8
BAYRIDGE 2	10.91	8.15	11.4	N/A
BAYRIDGE 3	8.34	5.63	8.54	6.2
BAYRIDGE 4	5.77	3.11	5.25	2.95

GROUND RESISTANCE (Ohms) = GPR / CURRENT

GRID SHAPE	TWO-LAYER MODEL		ALTERNATIVE 2-LAYER MODEL		MULTILAYER MODEL		MEASURED VALUES	
	CORNER MESH	CENTER MESH	CORNER MESH	CENTER MESH	CORNER MESH	CENTER MESH	CORNER MESH	CENTER MESH
BAYRIDGE 1	61	83.5	67	94.5	68	95.5	N/A	94
BAYRIDGE 2	70	52	87	63	83	65	N/A	N/A
BAYRIDGE 3	64	42	83	66	76	55	85	79
BAYRIDGE 4	31	13	40	24	37	23	41	25

TOUCH (MESH) VOLTAGES (in % of GPR)

∅ Corner Mesh Coordinates: X = 5.7', Y = 4.7'  
 - Corner Mesh Coordinates: X = 36', Y = 52'  
 # 25% measured is the average of 4 mesh values near the grid center. A fifth mesh voltage was also measured, but was suspiciously high and increases the average value to 33% when included with the 4 other values.

Center Mesh Coordinates: X = 108', Y = 118'

Table 3.2 Ground Grid Performance Results at Bayridge: Measured and Computed Results

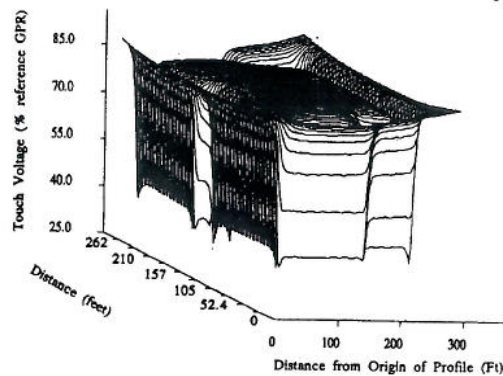


Figure 3.3 Touch Voltages (Bayridge, Stage 1)

It is clear from the preceding results that very good agreement exists between measured and computed results. Although soil resistivity results based on a six-layer earth model match much better the measured resistivity values than the two-layer model, the two-layer earth structure results still provide excellent agreement with observed ground grid performance. This is probably due to the fact that the six-layer model reflects soil structure characteristics outside the substation site while the two-layer model refers to the soil immediately surrounding the grounding grid. It is worthwhile noting at this point that it was not possible to derive a uniform soil model which would match both the GPR and earth potentials simultaneously. For example, a uniform soil assumption would result in a center mesh touch potential on the order of 60%, a value quite different from the 94% which was measured. Note that the two-layer computed value of 83.5% is still less in agreement with the measured value than the multilayer computed value of 95.5%.

Note that there is a large degree of uncertainty on the resistivity value of the bottom soil resistivity because the two-layer resistivity measurement traverse did not extend far enough. Values of 100 and 660 ohms-meters were determined from the multilayer and two-layer soil models, respectively. Because the multilayer traverse extended up to 100 feet, the bottom layers of the multilayer model were the basis for an estimated 200 ohm-meter alternative two-layer bottom soil resistivity.

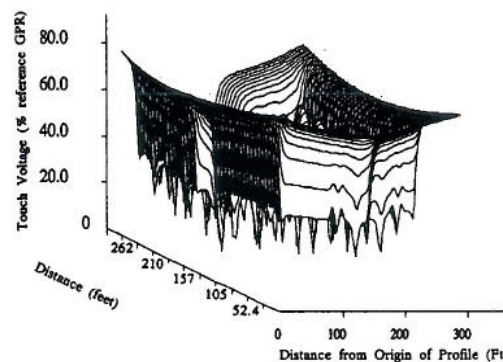


Figure 3.4 Touch Voltages (Bayridge, Stage 3)

These observations suggest the alternative two-layer soil model at the end of Table 3.1. This model provides excellent agreement with the measured resistance and touch voltage values. It is clear however that without the indications provided by the field measurements, only visual inspection of the resistivity curves suggests that further measurements at larger spacings are needed to remove the uncertainty on the resistivities of the lower layers (determination of the asymptotic value).

Finally, all measured resistance values are probably slightly below the exact values because the potential probe was placed at about 40% (i.e., 400') from the total distance to the return probe [6].

**3.2 WEST DAVENPORT SUBSTATION**

Figure 3.5 shows West Davenport substation ground system with all ground conductors installed. Field measurements were conducted first when only the perimeter ground wire was installed, then after installation of the remaining horizontal conductors and finally after driving four 100' ground rods at each corner of the grid. Note that one of the ground rods was driven in increments of 5 to 10 feet and resistance measurements were made as discussed below.

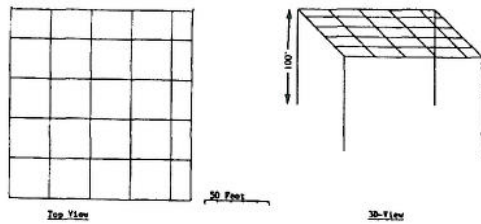


Figure 3.5 West Davenport Substation Grid; Final Stage of its Construction

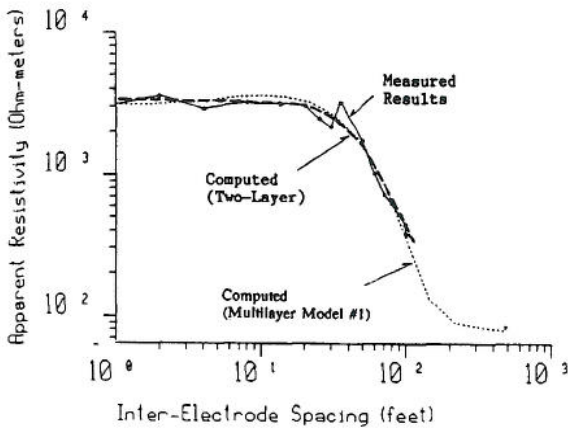


Figure 3.6 Measured and Computed Apparent Soil Resistivity at West Davenport Substation

The field and computed earth resistivity values are shown in Figure 3.6. Good agreement was obtained between the measured results and those calculated assuming a two-layer model and two five-layer models with the characteristics listed in Table 3.3.

SOIL TYPE	LAYER NO.	RESISIVITY (Ohm-m)	LAYER THICKNESS (Feet)
TWO-LAYER MODEL	1	3257	33.3
	2	157	-
MULTILAYER MODEL NO. 1	1	3100	3.3
	2	4000	10
	3	3000	23
	4	4000	10
	5	75	-
MULTILAYER MODEL NO. 2	1	3100	3.3
	2	4000	10
	3	3000	23
	4	1400	10
	5	124	-

Table 3.3 Best Fit Multilayer Model at West Davenport Substation

Table 3.4 summarizes the salient results obtained from the measurements and computations. Figures 3.7 and 3.8 are 3-D plots of the earth surface potentials which exist at the substation during a fault.

GRID SHAPE	TWO-LAYER MODEL	ALTERNATIVE MULTILAYER MODEL #1	MULTILAYER MODEL #2	MEASURED VALUES
DAVENPORT 1	31.9	35.0	34.9	32.3
DAVENPORT 2	17.2	20.3	20.3	17.0
DAVENPORT 3 100' RODS	2.6	1.5	2.4	2.9

GROUND RESISTANCE (Ohms) = GPR / CURRENT

GRID SHAPE	TWO-LAYER MODEL		MULTILAYER MODEL #1		MULTILAYER MODEL #2		MEASURED VALUES	
	CORNER MESH	CENTER MESH	CORNER MESH	CENTER MESH	CORNER MESH	CENTER MESH	CORNER MESH*	CENTER MESH
DAVENPORT 1	63	92	45	85.6	46	86	44	86
DAVENPORT 2	44	40	27	46	30	45	26	N/A
DAVENPORT 3 100' RODS	26	32	23	27	22	25	24	N/A

TOUCH (MESH) VOLTAGES (in % of GPR)

\* Center Mesh Coordinates: X = 108', Y = 108'  
 \* Corner mesh value is the average of the four corner mesh values

Table 3.4 Ground Grid Performance at West Davenport: Measured Values and Computed Results

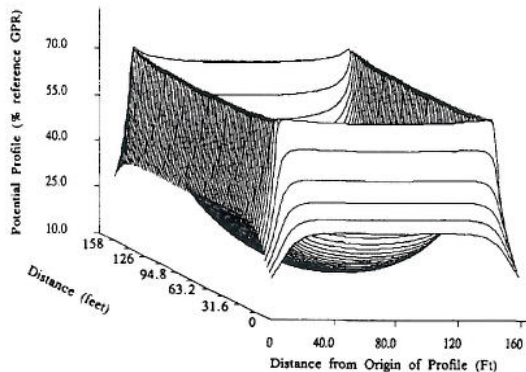


Figure 3.7 Earth Surface Potentials (West Davenport, 1 Mesh)

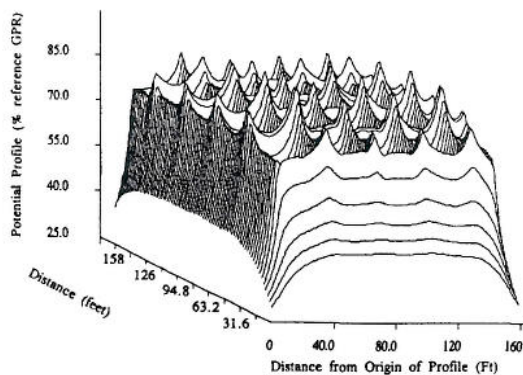


Figure 3.8 Earth Surface Potentials (West Davenport, Complete Grid)

Excellent agreement exists between the measured and computed values of substation ground resistance. It is worthwhile noting that both field measurements and computations indicated that the ground rods are highly effective in reducing the ground resistance only when more than 40 feet of each ground rod is driven in the soil: with four 25 foot long rods, the resistance drops marginally from 20.3 ohms (no rods) to 18.7 ohms. This is consistent with the soil structure model.

Note that the first corner ground rod was driven into the soil in increments of 5 feet initially and then in increments of 10 feet. The ground resistance of the rod was measured at each incremental step. For example, the resistance of the rod when driven 5 feet deep was 1815 ohms. It was 1852 ohms at 15 feet and about 2000 ohms at 20 feet: the resistance increased because of looser contact with the low resistivity top layer due to vibrations when driving the rod. The resistance dropped to 668 ohms at a 30 foot depth and to 56 ohms at a 40 foot depth. It then decreased gradually to reach 14 ohms at a 100 foot depth.

Good agreement is obtained between measured and computed touch voltages. Note however that the measured values represent the average values determined at the four corners. Because a portion of the West Davenport substation area was backfilled with a lower resistivity material than the virgin soil, differences on the order of 2 to 1 were observed for the measured touch voltages at the corners. Such differences could be approximated using vertical layers, as shown in the example in the next section.

Another cause of uncertainty in the measurement of touch voltages originates from the difficulty to determine accurately the location of an observation point with respect to the buried ground conductors.

### 3.3 VERTICAL LAYERS

As noted in the preceding paragraph, touch voltages are predominantly dependant on the local soil resistivity. Consequently, vertical discontinuities in the soil resistivity distort earth surface potentials. This is quite evident in Figure 3.10 which shows the earth surface potentials along the profile illustrated in Figure 3.9. This last figure presents an example grounding system located on the interface between two vertical layers of a 3-layer soil.

Vertical layers can also be useful to study grounding problems involving dams, beaches, lakes and valleys as well as modelling geological faults.

### CONCLUSIONS

Resistivities, ground resistances and touch voltages have been measured at two different substations. Field results reveal that because soil structures are highly nonuniform at both locations, it is not possible to select a uniform soil as a satisfactory model for predicting ground grid performance. A multilayer soil model however, yields accurate computation results.

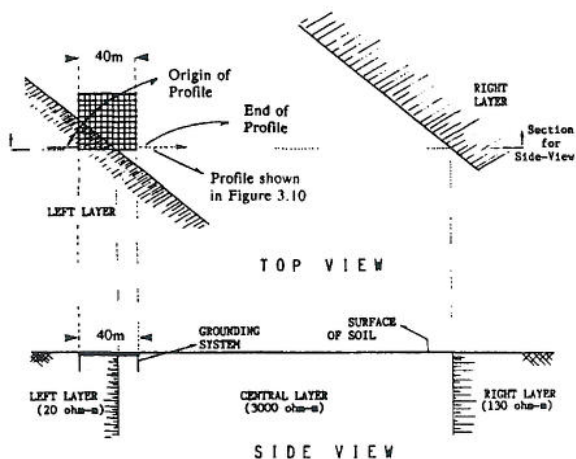


Figure 3.9 Grounding System Buried in a Vertically Layered Soil



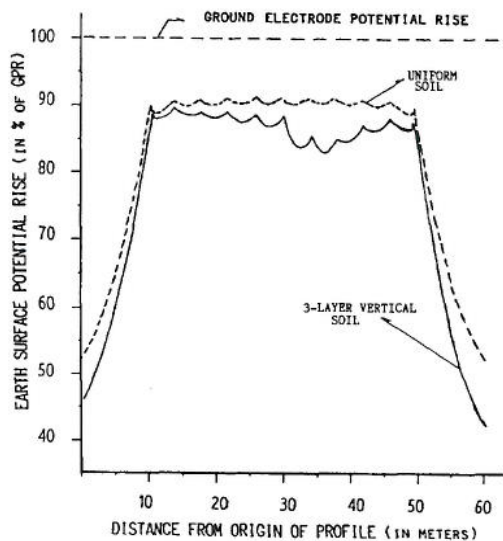


Figure 3.10 Distortion of Potential Profiles Due to Resistivity Discontinuity Across Vertical Layer Interfaces

Computations also indicate that vertical discontinuities have a noticeable impact on earth surface potentials and touch voltages. Measurements at locations where backfill was introduced (e.g., at the West Davenport substation) confirm this observation.

Finally, this work demonstrates clearly that precise and reasonably wide resistivity measurement traverses are indispensable to accurately predict ground grid performance in nonuniform soils. Long traverses are required to establish the asymptotic value of soil resistivity at depths on the order of grounding grid dimensions.

#### ACKNOWLEDGMENTS

This work was supported by Florida Power Corporation and Safe Engineering Services & technologies Ltd. The authors would like to thank Mr. R. K. Porter of FPC for his assistance during the measurements and Dr. Alan Selby and Mr. Robert Southey of SES for their constructive comments.

#### REFERENCES

- 1 - T.N. Giao, M.P. Sarma, "Effects of Two-Layers Earth on Electric Fields Near HVDC Electrodes", IEEE Trans., PAS-91, No.6, Nov. 72, pp. 2346-2355.
- 2 - F. Dawalibi, D. Mukhedkar, "Optimum Design of Substation Grounding in Two-Layer Earth Structure-Part I, Analytical Study," IEEE on PAS, Vol. PAS-94, No.2, March/April 1975, pp. 252-261.
- 3 - F. Dawalibi, D. Mukhedkar, "Optimum Design of Substation Grounding in Two-Layer Earth Structure - Part II and Part III". IEEE Trans. on PAS, Vol. PAS-94, No.2, March/April 1975, pp. 262-272.
- 4 - R.J. Heppel, "Computation of Potential at Surface Above an Energized Grid or Other Electrode, Allowing for Non-Uniform Current Distribution", IEEE Trans., PAS-98, No.6, Nov./Dec. 79, pp. 1978.
- 5 - A.P. Meliopoulos, R.P. Webb, E.B. Joy, "Analysis of Grounding Systems." IEEE Trans., PAS-100, No.3, March 81, pp. 1039-1048.
- 6 - F. Dawalibi, D. Mukhedkar, "Parametric Analysis of Grounding Grids", IEEE Trans. on PAS, Vol. PAS-98, No.5, Sept./Oct. 1979, pp. 1659-1668.
- 7 - F. Dawalibi, D. Mukhedkar, "Influence of Ground Rods on Grounding Grids." IEEE Trans. on PAS, Vol. PAS-98, No.6, Nov./Dec. 1979, pp. 2089-2098.
- 8 - F. Dawalibi, D. Mukhedkar, D. Bensted, "Measured and Computed Current Densities in Buried Ground Conductors", IEEE Transactions on PAS, Vol. PAS-100, No.8, August 1981, pp. 4083-4092.
- 9 - D.G. Kasten, R. Caldecott, "Substation Grounding Scale Model Tests", EPRI Research Report, EL-3099, Project 1494-3, May 1983.
- 10 - F. Dawalibi, "Transmission Line Grounding", EPRI Research Report, Project 1494-1, Vol. 1 and 2, August 1982.
- 11 - E.A. Cherney, K.G. Ringler, N. Kalcio, G.K. Bell, "Step and Touch Potentials at Faulted Transmission Towers", IEEE Trans., PAS-100, No.7, July 1981, pp. 3312-3321.
- 12 - "IEEE Guide for Safety in AC Substations", ANSI/IEEE Std. 80, 1986.
- 13 - P.J. Lagacé, J.L. Houle, Y. Gervais, D. Mukhedkar, "Evaluation of the Voltage Distribution Around Toroidal HVDC Ground Electrodes in N-Layer Soils". IEEE Trans. on PWRD, Vol. 3, No. 4, October 1988, pp. 1573-1577.
- 14 - P.J. Lagacé, D. Mukhedkar, H.H. Hoang, H. Greiss, "Evaluation of the Effect of Vertical Faults on the Voltage Distribution around HVDC Electrodes using a Supercomputer", IEEE Trans. on PWRD, Vol. 5, No. 3, July 1990, pp. 1309-1313.
- 15 - S.S. Stefanescu, C. & M. Schlumberger, "Sur la Distribution Electrique Potentielle Autour d'une Prise de Terre Ponctuelle dans un Terrain à Couches Horizontales Homogènes et Isotropes", Journal de Physique et Radium, vol.1. Serie VII, No. 4, 1930, pp. 132-140.

- 16- H.H. Mooney, E. Orellana, H. Pickett, L. Tornheim, "A Resistivity Computation Method for Layered Earth Models", *Geophysics*, Vol. XXXI, No. 1, February 1966, pp. 192-203.
- 17- H. Flathe, "A Practical Method of Calculating Geoelectrical Model Graphs for Horizontally Stratified Media", *Geophysical Prospecting*, Vol. 3, pp. 268-294.
- 18- F. Dawalibi, C.J. Blattner, "Earth Resistivity Measurement Interpretation Techniques", *IEEE Trans. on PAS*, Vol. PAS-103, Number 2, February 1984, pp. 374-382.
- 19- T. Takahashi, T. Kawase, "Analysis of Apparent Resistivity in a Multi-Layer Earth Structure", *IEEE Trans. on PWRD*, Vol. 5, no. 2, April 1990, pp. 604-612.
- 20- G.V. Keller, F.C. Frischknecht, "Electrical Methods in Geophysical Prospecting", Pergamon Press. New York (1977).
- 21- A.B. Oslon, I.N. Stankeeva, "Application of Optical Analogy to Calculation of Electric Fields in Multi-Layer Media", *Electric Technology U.S.S.R.*, No. 4, 1979, pp. 68-75.
- 22- D.P. Ghosh, "The Application of Linear Filter Theory to the Direct Interpretation of Geoelectrical Resistivity Grounding Measurements", *Geophysical Prospecting* 19, 1971, pp. 192-217.
- 23- F. Dawalibi, A. Selby, "Electromagnetic Fields of Energized Conductors", Companion Paper Submitted to IEEE PWRD Winter Power Meeting, 1991.
- 24- N. Barbeito, "Substation Ground Grid Tests", IEEE Southeastern Electric Exchange Conference, June 2, 1988.

Dr. Farid Dawalibi (M'72, SM'82) was born in November, 1947. He received a Bachelor of Engineering degree from St. Joseph's University, affiliated with the University of Lyon, and the M. Sc. A. and Ph. D. degrees from Ecole Polytechnique of the University of Montreal. From 1971 to 1976, he worked as a consulting engineer with the Shawinigan Engineering Company, in Montreal. He worked on numerous projects involving power system analysis and design, railway electrification studies and specialized computer-software code development. In 1976, he joined Montel-Sprecher & Schuh, a manufacturer of high voltage equipment in Montreal, as Manager of Technical Services and was involved in power system design, equipment selection and testing for systems ranging from a few to several hundred kV.

In 1979, he founded Safe Engineering Services & Technologies, a company which specializes in soil effects on power networks. Since that time he has been responsible for the engineering activities of the company including the development of software code related to power systems applications.

He is the author of more than sixty papers on power systems grounding and safety, soil resistivity, electromagnetic interference. He has written several research reports for CEA and EPRI.

Dr. Dawalibi is a corresponding member of various IEEE Committee Working Groups, and a senior member of the IEEE Power Engineering Society and the Canadian Society for Electrical Engineering. He is a registered Engineer in the Province of Quebec.

Mr. Nelson Barbeito (M'84) was born on March 8, 1946. He received his B.S. degree in Electrical Engineering from Christian Brothers College in Memphis, Tennessee in 1968. In 1969 he joined Florida Power Corporation as an engineer in the Substation Design Department. He has worked in the areas of Substation Design, Relay Design and in the Substation Maintenance and Testing Departments. Mr. Barbeito is presently a Senior Engineer in the Transmission and Substation Engineering Services Department. Mr. Barbeito's main technical interests are in power system protection, grounding and interference analysis. He has published several papers on these topics. Mr. Barbeito is a member of the IEEE Substation Committee and serves in several working groups.

### Discussion

**D. W. Jackson** (R. W. Beck and Associates, Waltham, MA): The use of the term "vertical layer" is misleading and confusing. The root meaning of the word is to lay flat. The inherent meaning of the word is essentially horizontal, though there may be sloped layers, tapered layers or up-turned layers. It would be desirable to adopt a more generally descriptive term. For this purpose a "vertical discontinuity" or a "horizontal non-uniformity" might be used, since horizontal layers of differing resistivities constitute vertical non-uniformities. The practice of soil resistivity measurement and description is lacking a good descriptive term for the vertical interface between two soil masses with differing characteristics.

**D. N. Laird** (Los Angeles Department of Water and Power): This paper is valuable to the Industry in that it combines detailed field measurements with calculated values based on two-layered and multi-layered soils.

In Figure 3.2 it appears that the two-layer computed values match fairly closely to the 1988 measurements. Which set of resistivities and layer thicknesses are used in the two-layer computed value?

How many soil resistivity measurements did the authors take in 1988 at Bayridge and how many more in 1989.

The difference between West Davenport 2 and 3 is the addition of four 100-foot-long ground rods. The paper shows that the measured resistance was lowered from 17 ohms to 2.9 ohms, which is 5 1/2 times lower!, however the corner mesh GPR only changed from 26% to 24% GPR. Can the authors give some calculation of the total GPR at West Davenport 2 and West Davenport 3 and show the effect of the lower resistance at West Davenport 3?

**F. Dawalibi, N. Barbeito**: The authors would like to thank the discussers for their comments.

The authors agree that the term "vertical layer" can be confusing. It is, however, widely used and is consistent with the "horizontal" qualifier used to define the more usual type of layering. The term "vertical fault"

or simply "fault" is often used by geophysicists to designate an abrupt variation of resistivity in a horizontal direction.

The West Davenport site was on a small hill, thus requiring a partial fill for leveling. This resulted in a "vertical layer". Viewed from the side of the substation, the line of sight would traverse two soil masses positioned next to each other. The interface between the two is a vertical surface and therefore suggests use of the term "vertical layer".

The 1988 resistivity test was performed within the substation grid area before the wires were installed. The 1989 resistivity test was performed just outside the grid area after the substation was in service. The additional test in 1989 was required to obtain deeper soil information for increased computer modelling accuracy: the soil resistivity at depths of 70 m or more would otherwise have remained uncertain because the 1988 measurements did not extend far enough.

The resistivity values used in the calculations are indicated in Table 3.1. The alternative 2-layer model is based on interpretation of the 1988 two-layer soil measurements, except that the bottom soil resistivity has been replaced with an average value based on information extracted from the 1989 multi-layer results. Since soil resistivity at large depths (greater than 50 m) is not sensitive to varying weather conditions, the 1989 resistivity information is considered an accurate source for establishing an equivalent bottom layer resistivity.

The mesh voltage at the corner mesh, expressed as a percentage of the grounding system GPR, decreased from 26% to 24%. Each of these percentages, however, applies to a different GPR value. The measured mesh voltage, when expressed as an absolute value, was reduced from 9.8 volts to 2.0 volts by the addition of the four ground rods. Table 1 of Reference 1 below lists the actual field measurement.

### Reference

1. J. Lazzra, N. Barbeito, "Simplified Two Layer Model Substation Ground Grid Design Methodology," IEEE Paper No. 90 WM 131-3 PWRD.

Manuscript received June 12, 1991.

## BEHAVIOUR OF GROUNDING SYSTEMS IN MULTILAYER SOILS: A PARAMETRIC ANALYSIS

F. P. Dawalibi, Senior Member, IEEE    J. Ma, Member, IEEE    R. D. Southey, Member, IEEE

Safe Engineering Services & technologies ltd  
1544 Viel, Montreal, Canada, H3M 1G4

**ABSTRACT:** *An extensive parametric study of grounding grid performance in multilayer soil structures has been carried out for the first time. Various practical cases have been examined and the corresponding grounding grid resistances, current distributions, earth surface potentials and touch voltages have been presented and compared for different soil structures. The results presented in this paper provide a benchmark for future work in this domain. They also illustrate practical situations, such as frozen or partially frozen soil conditions, which has remained an open question to date, in which the multilayer structure of the soil must be considered if a safe grounding system design is to be achieved.*

**Keywords:**

safety, grounding, foot resistance, frozen soil, resistivity

### 1. INTRODUCTION

Grounding grid performance, which can be measured in terms of ground resistance, touch voltages and step voltages, is heavily dependent on soil structure. Although two layer soil models can represent the real soil structure in some cases, the use of multilayer soil models is unavoidable to accurately model most soil structures. Some representation of the soil structure is usually taken into account at the time a grid is designed. However, the top soil characteristics can vary significantly even after the grid is installed. For example, the resistivity of surface soil can increase by as much as two orders of magnitude when the soil freezes and it is also sensitive to the moisture content of the soil [1,2]. The same is also true for crushed rock and concrete. The behaviour of grounding systems in soils in various states of freezing has remained an open question to date. Therefore, it is desirable to study the effect of top soil resistivity variations on the performance of grounding systems of various types.

An extensive parametric analysis of grounding grids in uniform and two-layer soils has been carried out by Dawalibi and Mukhedkar [3]. The comparison between measured and computed current densities in buried ground conductors in uniform and two-layer soils was made a decade ago [4]. Foot resistances in two-layer and multilayer soils have been studied [5,6] and some measurements and computations related to grounding systems buried in multilayer soils are also available [7]. In this paper, a detailed parametric analysis of grounding networks

in multilayer soil (more than two layers) is carried out for the first time. In particular, we focus our attention on the effects of multilayer soil structure variations on the performance of several grounding grid configurations. In the latter part of this paper, the effects of soil freezing and thawing are discussed.

### 2. BRIEF DESCRIPTION OF THE ANALYTICAL APPROACH

The numerical results presented here are based on the method of images for multilayer soil following the technique developed by Oslon and Stankeeva [8]. See also Dawalibi and Barbeito [7] for a discussion on various multilayer analytical approaches (and successful comparison between measured and computed results) and Chow *et al.* [9] for a theoretical discussion on an algorithm to accelerate computations involving multilayer soils. For a given multilayer soil, a base thickness value is found and all layer thicknesses are expressed as a multiple of this base value. It should be noted that in [8], only the case of a point current source located on the earth surface is analyzed. When the source is at a certain depth, the authors of [8] states that the base value is the overall measure (largest common divisor) of all the layer thicknesses and the depth of the current source. In this case it is impossible to analyze other sources such as a vertical or slant line current because different points on the line source have different depths. However, by rearranging the starting point for the image generation, it is relatively easy to select a base value which is independent of the depth of the current source. Hence, an expression for the potential due to a point current source buried at any depth in a multilayer soil is obtained. Subsequently, the potential due to a current leaking out from a short conductor segment can be obtained by direct integration. For a grounding network, the current distribution has to be determined first. The commonly used technique is the Method of Moments, which requires, in this case, the subdivision of conductor network, choosing basis functions and setting up and solving a set of linear equations.

It should be noted that the method of images described in [8] and used by the authors is different from that proposed in [10,11], which requires the generation of a large number of images to achieve a satisfactory accuracy. Indeed, because the layer thicknesses are a multiple of a common base value, the image generation process used to conduct the parametric analysis in this paper is considerably simpler and more efficient. Also, once the images are generated, they are used in determining both the current distribution and the earth potentials. Hence the computation time is quite reasonable, i.e., usually 2 to 10 times that required for a uniform soil.

93 WM 122-2 PWRD A paper recommended and approved by the IEEE Substations Committee of the IEEE Power Engineering Society for presentation at the IEEE/PES 1993 Winter Meeting, Columbus, OH, January 31 - February 5, 1993. Manuscript submitted August 25, 1992; made available for printing January 6, 1993.

### 3. PARAMETRIC ANALYSIS

In this analysis, four representative multilayer soil structure models are considered. The first model consists of a low resistivity layer sandwiched between two high resistivity layers. The second model consists of a high resistivity layer sandwiched between two low resistivity layers. The third model consists of a high resistivity surface soil gradually decreasing in resistivity with increasing depth. The fourth model consists of a low resistivity surface soil gradually increasing in resistivity with increasing depth. Table 1 presents all the parameters of these four soil structures. In these models, all the layer thicknesses are assumed equal for simplicity. Nonequal thicknesses are as easily handled as shown in the practical examples in Section 4.2.

Model	Layer	Resistivity ( $\Omega\text{-m}$ )	Thickness (meters)
(a)	1	2000	3.0
	2	100	3.0
	3	1000	$\infty$
(b)	1	50	3.0
	2	1000	3.0
	3	100	$\infty$
(c)	1	1000	2.0
	2	750	2.0
	3	500	2.0
	4	250	2.0
	5	150	2.0
	6	100	$\infty$
(d)	1	100	2.0
	2	150	2.0
	3	250	2.0
	4	500	2.0
	5	750	2.0
	6	1000	$\infty$

Table 1 Layer Characteristics of Soil Structures Studied  
The grounding grids modelled in this study are the following:

- S1 - 20 m  $\times$  20 m square one-mesh grid;
- S4 - 20 m  $\times$  20 m square four-mesh grid;
- S16 - 20 m  $\times$  20 m square sixteen-mesh grid;
- S64 - 20 m  $\times$  20 m square sixty-four-mesh grid.

#### 3.1. Current Distribution in Grounding Networks

The current density distribution (current per meter of conductor length leaking into the earth) is plotted for different scenarios in Figures 1, 2, 3, 4 and 5. Grid types S1, S4 and S16 were studied in this part of the analysis. The current injected into the three types of grids was maintained proportional to the total conductor length in each grid, i.e.,  $4 \times 100 \text{ A} = 400 \text{ A}$  for S1,  $6 \times 100 \text{ A} = 600 \text{ A}$  for S4, and  $10 \times 100 \text{ A} = 1000 \text{ A}$  for S16. Hence if the current were distributed uniformly in all conductors, the current density would be 5 A/m. Figures 1 and 2 show the current density functions when an S1 grid is buried in soil models (a) and (b), respectively, at different depths. It can be seen that

except for one curve, all the curves are rather flat, which implies that the current distribution is fairly uniform. In Figure 1, the curve with the largest variation represents the current density when the grid is buried 4.5 meters deep. In Figure 2, the curve with the largest variation represents the current density when the grid is buried 1.5 meters deep. In both cases, the grid is buried in the low resistivity layer and the current density is larger at the conductor ends than in the middle. This is because the current tends to flow laterally away from the grid center rather than downwards, due to the presence of a high resistivity layer beneath the low resistivity layer. When the grid is in the high resistivity layer, the opposite is true, though in this case the variation of the current density along each conductor is relatively small. When the burial depth of the grid becomes very large, the current density is almost uniform in both soil structures because the influence of the top layers is very small and the square loop behaves much like a circular loop would.

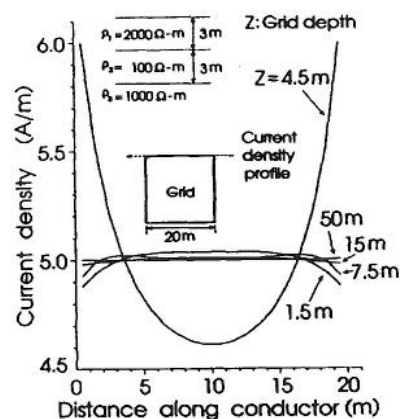


Figure 1 One-Mesh Grid Current Density in Soil Model (a) at Various Grid Depths.

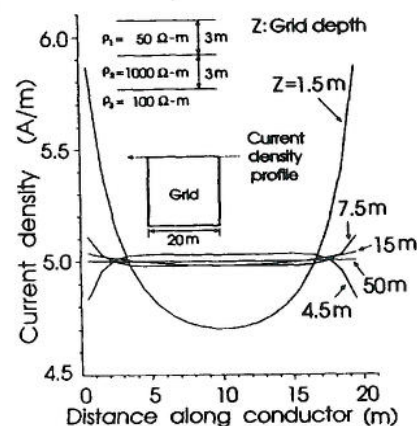


Figure 2 One-Mesh Grid Current Density in Soil Model (b) at Various Grid Depths.

Figure 3 shows the current density along a center conductor and a perimeter conductor of an S4 grid buried at various depths in soil model (a). It can be seen that at nodes of the grid, the current density is low. The current density along the center conductor is generally lower than that along the perimeter conductor. It is interesting to see that when the grid is buried in a low resistivity layer, the current density along the center conductor is the lowest while that along the perimeter conductor is the highest. This again indicates that the current tends to flow laterally rather than downwards when the grid is in the low resistivity layer. Figure 4 shows the current density along a perimeter conductor of an S16 grid buried at different depths in soil model (b). The ripples in the current distribution are due to the presence of several nodes in the grounding grid.

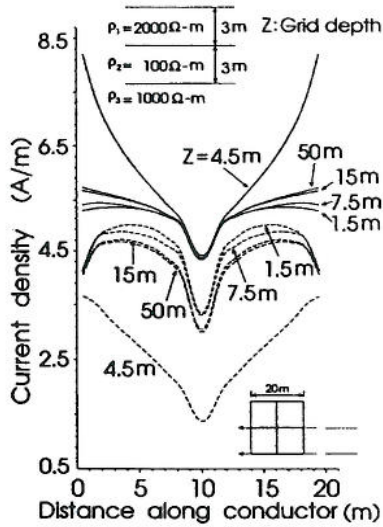


Figure 3 Four-Mesh Grid Current Density in Soil Model (b) at Various Grid Depths.

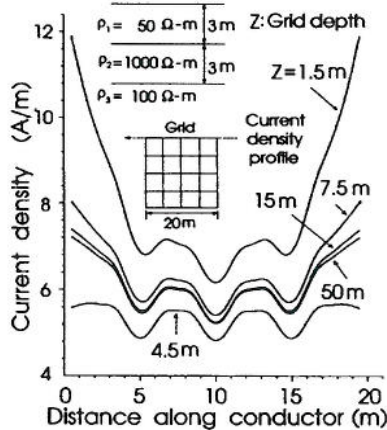


Figure 4 Sixteen-Mesh Grid Current Density in Soil Model (a) at Various Grid Depths.

In Figure 5, the current density along a conductor of an S1 grid buried at various depths in soil model (d) is presented. Since the resistivity increases with increasing depth, the variation in current density with depth is expected and is explained by the foregoing discussion. The current density functions corresponding to small grid depths have larger values at the extremities than in the middle. As the grid depth increases, the current distribution curves have larger values in the middle than at the extremities and little variation occurs. When the grid is very deep, the current density distribution is close to that of a ring electrode which is uniform because of symmetry.

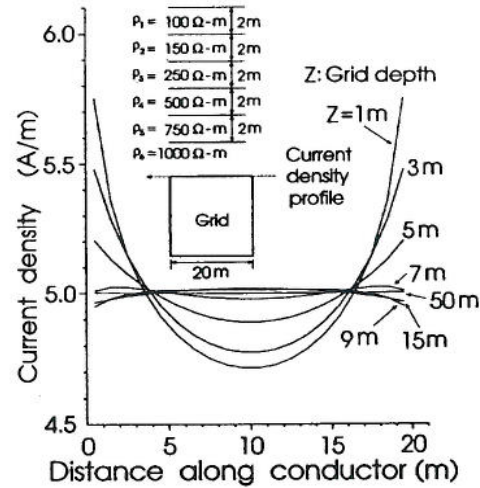


Figure 5 One-Mesh Grid Current Density in Soil Model (d) at Various Grid Depths.

### 3.2. Earth Surface Potentials and Touch Voltages

Figure 6 shows the earth surface potentials due to four different grids buried 0.5 meter deep in soil model (c) with 1000 A injection current. The increase in the number of conductors in the grid increases the minimum earth potentials above the grid and makes the earth potentials more evenly distributed. The ground potential rise (GPR) of the grid also decreases because the ground resistance is decreased. As a result, the touch voltages decrease. Figure 7 shows the touch voltages corresponding to Figure 6. The earth surface potentials due to an S16 grid buried in soil model (b) at different depths are shown in Figure 8. In a uniform soil, the increase of the grid depth results in a simultaneous decrease of the grid potential rise and the earth surface potentials [3], while in the multilayer case, this is not always true. The increase of the grid depth will always result in a decrease of the earth surface potentials. The grid potential rise, however, can increase or decrease significantly, depending upon whether the grid is in a high or low resistivity layer. The three curves with the highest magnitudes in Figure 8 correspond to grid depths of 0.1 m, 0.5 m and 1.5 m, respectively. The grid is in the top low resistivity layer in these three cases. The differences in the

magnitudes of the earth surface potentials in these three cases are also relatively small. The GPRs in these three cases are: 2.65 kV, 2.57 kV and 2.51 kV, respectively. Again the differences are small, as expected. The earth surface potential curve corresponding to the grid depth of 4.5 m is substantially lower than the curves corresponding to the depths of 0.1 m, 0.5 m and 1.5 m. The GPR in this case is 6.15 kV, much higher than for the smaller depths. As a result, the touch voltage increases markedly. The touch voltage curves corresponding to Figure 8 are shown in Figure 9.

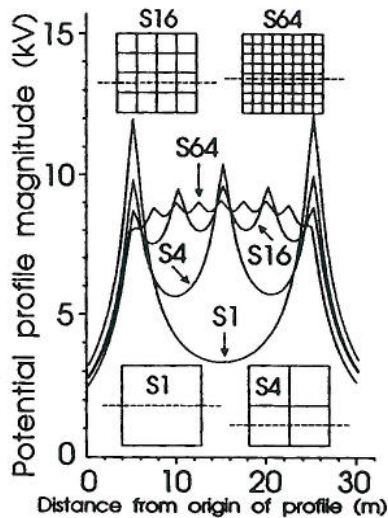


Figure 6 Earth Surface Potentials Due to Various Grids in Soil Model (c).

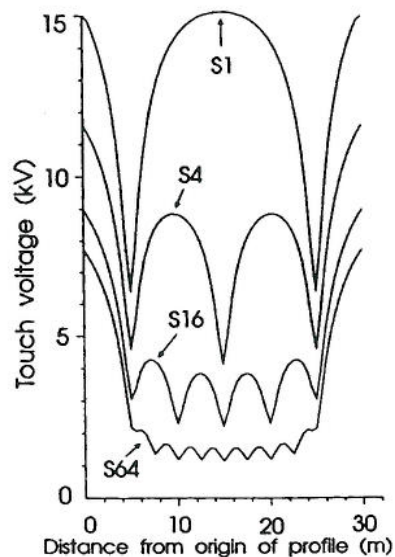


Figure 7 Touch Voltages Due to Various Grids in Soil Model (c).

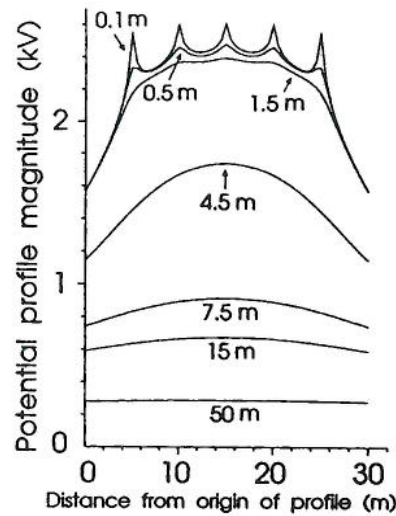


Figure 8 Earth Surface Potentials Due to an S16 Grid in Soil Model (b) at Various Grid Depths.

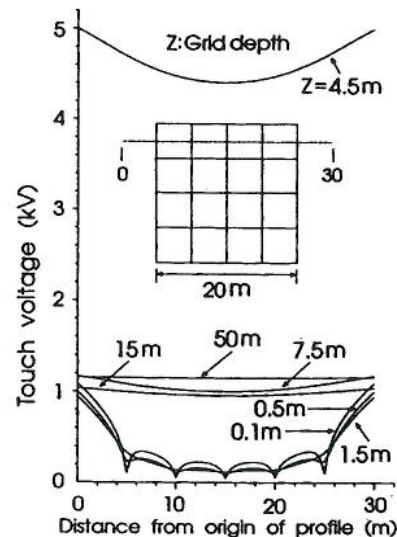


Figure 9 Touch Voltages Due to an S16 Grid in Soil Model (b) at Various Grid Depths.

### 3.3. Ground Resistances

Ground-resistances for grid types S4 and S16 buried at various depths in different soils are presented in Tables 2 and 3. It can be seen that the resistance values are greatly dependent on the layer in which the grid is located. When it is located in a low resistivity layer, the ground resistance is low. In the case of uniform soil, when the depth of a grid increases, the ground resistance decreases. In the case of multilayer soil, this is not always true, even if the change of grid depth is confined within one layer. Consider the case of

grid type S4 buried in soil model (a), for example. The ground resistance value is 14.63  $\Omega$  when the depth of the grid is 7.5 meters and 16.16  $\Omega$  when it is 15 meters. The resistance value keeps increasing even when the depth of the grid is 50 meters. The reason for this behavior is that as the grid depth increases, the influence of the low resistivity layer decreases. When the grid is deep enough so that the influence of the low resistivity layer is negligible, we expect the resistance value to reach a maximum and then begin to decrease. This is confirmed by the resistance calculation for the case when a grid of type S4 is buried in soil model (a) at a depth of 100 meters. The resistance is 13.86  $\Omega$ , which is smaller than that for the case when the depth of the grid is 50 meters, in which case the resistance is 16.32  $\Omega$ .

In Table 3, the ground resistance value decreases rapidly with increasing grid depth in the case of soil model (c) because of the low resistivity of the deeper layers. The ground resistance value increases with increasing grid depth in the case of soil model (d) because the resistivity values are higher in the deeper layers. We also expect a maximum ground resistance value at a certain depth and the resistance will decrease with increasing grid depth after this critical depth has been attained.

Depth (m)		Ground Resistance ( $\Omega$ )			
		Grid Type: S4		Grid Type: S16	
		Soil Model			
Layer	(a)	(b)	(a)	(b)	
1.5	1	24.46	2.57	19.40	2.51
4.5	2	7.99	8.67	7.86	6.15
7.5	3	14.63	2.13	12.23	1.91
15.0	3	16.16	1.85	13.86	1.63
50.0	3	16.32	1.66	14.05	1.43

Table 2 Ground Resistances of S4 and S16 Grids Buried at Various Depths in Type (a) and (b) Soil Structures.

Depth (m)		Ground Resistance ( $\Omega$ )			
		Grid Type: S4		Grid Type: S16	
		Soil Model			
Layer	(c)	(d)	(c)	(d)	
1.0	1	12.95	7.01	10.48	6.86
3.0	2	9.03	7.24	7.24	6.98
5.0	3	6.06	8.01	4.87	7.50
7.0	4	3.70	9.99	3.12	8.85
9.0	5	2.67	12.24	2.34	10.47
15.0	6	1.97	15.48	1.75	13.16
50.0	6	1.67	16.21	1.45	13.94

Table 3 Ground Resistances of S4 and S16 Grids Buried at Various Depths in Type (c) and (d) Soil Structures.

It should be noted that the large depth values provide computation results for scenarios involving conductors buried in the various layers of a multilayer soil, while giv-

ing a clear indication of the asymptotic trends due to wide variations in some key parameters. The trends will remain similar, although not identical, if the grid depths and the layer thicknesses are divided by a constant. If, in addition, the grid dimensions are also divided by this constant, all results will still apply if they are multiplied by the constant.

#### 4. PRACTICAL CASES

In this section, we will examine the behaviour of grounding system resistances, foot resistances and touch voltages in several practical situations which involve multilayer soil structures.

##### 4.1. Frozen Soil

When the temperature is below freezing, the resistivity of the soil close to the earth surface increases rapidly as the temperature drops. A soil which is initially uniform, with a resistivity of 100  $\Omega$ -m, may exhibit a multilayer structure with the resistivity of its top layer as high as 10000  $\Omega$ -m, when it freezes. Table 4 lists the layer thicknesses and resistivities of two representative frozen soil structures corresponding to a soil which is uniform, with a resistivity of 100  $\Omega$ -m when no freezing has occurred.

Model	Layer	Resistivity ( $\Omega$ -m)	Thickness (meters)
(e) Winter	1	2000	0.2
	2	1500	0.2
	3	1000	0.2
	4	500	0.2
	5	250	0.2
	6	100	$\infty$
(f) Spring	1	100	0.2
	2	500	0.2
	3	1000	0.2
	4	500	0.2
	5	250	0.2
	6	100	$\infty$

Table 4 Two Soil Structures Corresponding to Frozen Condition of 100  $\Omega$ -m Uniform Soil.

Model (e) simulates the soil in mid-winter and model (f) in early spring. Consider a 20 m  $\times$  20 m 16-mesh grid buried at at depth of 0.45 meter with a 1000 A fault current injected into the grid. Figure 10 shows the resulting earth surface potentials along a profile traversing the grid, for soil models (e) and (f) and for a uniform soil with a resistivity of 100  $\Omega$ -m. It can be seen that the earth surface potentials for soil models (e) and (f) are much higher than for the uniform soil. Figure 11 shows the touch voltages for the three soil models along the same profile. The touch voltage and the foot resistance are key elements for the calculation of body currents. From Figure 11, it can be seen that the touch voltages over the grid area in Cases (e) and (f) are about 10 times higher than in the case of the non-freezing uniform soil (i.e., over 2200 volts versus 220 volts).



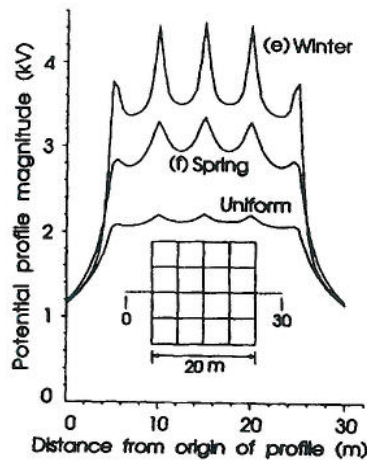


Figure 10 Earth Surface Potentials Over a 16-Mesh Grid in Soil Experiencing Varying Degrees of Freezing.

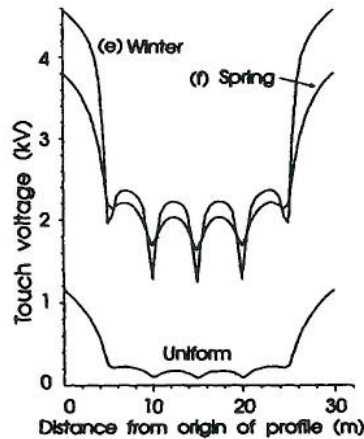


Figure 11 Touch Voltages Over a 16-Mesh Grid in Soil Experiencing Varying Degrees of Freezing.

The foot resistances calculated using the Thevenin equivalent impedance method described in [5], the touch voltages in the grid area of the earth surface and ground resistance of the grid for the three soil models are listed in Table 5.

Model	Ground Resistance (Ω)	Foot Resistance (Ω)	Touch Voltage (volts)
Uniform	2.31	156.2	220
(e) Winter	5.73	2928.5	2380
(f) Spring	4.99	214.9	2200

Table 5 Variations in Grid Resistance, Foot Resistance and Maximum Touch Voltage as a Function of Degree of Soil Freezing.

For soil model (e), although the touch voltage increases by a factor of 11, the foot resistance increases even more (by a factor of 19 in this case). A different pattern is displayed by soil model (f), for which the foot resistance increases only slightly while the touch voltage increases by a factor of 10. This raises the question of safety in this situation. The addition of ground rods will increase the safety and robustness of the grounding system design, as will be seen in the following. Note that the ground resistances also change for the frozen soil in both cases.

Let us now consider the case when an S16 grid with ground rods as shown in Figure 12 is buried in soil structures given in Table 4 and in a 100 Ω-m uniform soil. The ground resistances and touch voltages are listed in Table 6. It can be seen that the addition of ground rods reduces the touch voltages for the cases of soil models (e) and (f) by half. The ground resistances for the two cases are also substantially decreased. By contrast, the addition of rods has a smaller effect on the grounding grid performance for the case of uniform soil.

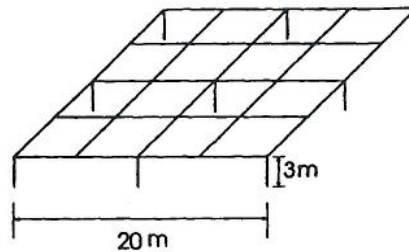


Figure 12 A 16-Mesh Grid with Ground Rods.

Model	Ground Resistance (Ω)	Touch Voltage (volts)
Uniform	2.16	180
(e) Winter	3.55	1080
(f) Spring	3.35	1100

Table 6 Grid Resistances and Touch Voltages for the Case of a Grid with Ground Rods.

#### 4.2. Frozen Soil with Crushed Rock Covering Layer

Three different soil models are shown in Table 7. Soil model (g) represents a uniform soil of 100 Ω-m covered by a 0.2 meter thick layer of crushed rock with a resistivity of 1000 Ω-m. Soil model (h) represents the same soil during mid-winter freezing, which increases the resistivities of the gravel and the top 0.5 meter of surface soil by a factor of 10 and the next 0.5 meter of soil by a factor of 2. Soil model (i) represents the soil during early spring when it has started to thaw. Here, only the crushed rock layer has thawed, while the surface soil remains frozen as in model (h).

Model	Layer	Resistivity ( $\Omega$ -m)	Thickness (meters)
(g)	1	1000	0.2
	2	100	$\infty$
(h)	1	10000	0.2
	2	1000	0.5
	3	200	0.5
	4	100	$\infty$
(i)	1	1000	0.7
	2	200	0.5
	3	100	$\infty$

Table 7 Parameters of Three Soil Structures Modelled in Various States of Freezing with a Crushed Rock Covering Layer.

The grid ground resistances, foot resistances and maximum touch voltages for the three soil models shown in Table 7 are presented in Table 8. When the resistivities of both the crushed rock and the top soil increase (i.e., winter conditions), the touch voltage increases by a factor of 10.5, while the foot resistance increases by a factor of 10. As a result, safety is almost not affected. On the other hand, when the resistivity of the crushed rock remains constant while that of the top soil increases due to freezing (i.e., early spring conditions), the touch voltage increases by a factor of 8 and the foot resistance increases by only 20%. In this situation, a grid design that is satisfactory in winter and in summer may become unsatisfactory in early spring. The presence of ground rods will typically increase the safety and robustness of the grounding system design as can be seen in Section 4.1.

Model	Ground Resistance ( $\Omega$ )	Foot Resistance ( $\Omega$ )	Touch Voltage (volts)
(g)	2.30	1306.8	240
(h)	4.51	13053.1	2520
(i)	4.48	1580.8	1930

Table 8 Variations in Grid Resistance, Foot Resistance and Maximum Touch Voltage as a Function of Degree of Soil Freezing, with Crushed Rock Layer Present.

#### 4.3. Crushed Rock Surface with a Thin Layer of Mud

High resistivity crushed rock is widely used in practice in order to increase foot resistance. However, the resistivity of the crushed rock may decrease due to contamination, as discussed in [6]. Here we consider another scenario in which the crushed rock is covered by a thin layer of water or residue such as mud or clay. When a thin layer of mud is on top of soil model (g) in Section 4.2, the soil model shown in Table 9 results.

Layer	Resistivity ( $\Omega$ -m)	Thickness (meters)
1	50	0.05
2	1000	0.2
3	100	$\infty$

Table 9 Soil with Crushed Rock Layer Covered by Thin Layer of Mud.

The corresponding results are shown in Table 10.

Ground Resistance ( $\Omega$ )	Foot Resistance ( $\Omega$ )	Touch Voltage (volts)
2.28	219.8	270

Table 10 Grid Ground Resistance, Foot Resistance and Maximum Touch Voltage Resulting from Soil with Crushed Rock Layer Covered by Thin Layer of Mud.

It can be seen that the touch voltage increased as compared to the case of soil model (g) in Section 4.2 and the foot resistance decreases markedly from 1306.8  $\Omega$  to 219.8  $\Omega$ . This results in a significant rise of body currents (typically, a 100% increase).

## 5. CONCLUSIONS

An extensive study of grounding grid performance in different multilayer soils has been carried out. Various practical cases have been examined and the variations of grounding grid resistance, current distribution, earth surface potentials and touch voltages have been presented and compared for different soil structures. The results presented in this paper can be used as a benchmark for reference in future studies in this area. Examples have also been presented showing how the safety performance of a grounding system is influenced by various types of freezing and by the presence of low resistivity top soil layers caused by rain.

## 6. ACKNOWLEDGMENTS

The authors wish to thank Safe Engineering Services & technologies for the financial support and facilities provided during this research effort.

## 7. REFERENCES

- [1] P. Hoekstra and D. McNeill, "Electromagnetic Probing of Permafrost", Sec. Int. Conf., North American Contribution, NAS, 1973, pp. 517-526.
- [2] "Earth Resistivities of Canadian Soils", Research Report, Canadian Electrical Association, July 1988.
- [3] F. P. Dawalibi and D. Mukhedkar, "Parametric Analysis of Grounding Grids", IEEE Trans. on PAS Vol. 98, No. 5, Sept.-Oct. 1979, pp. 1659-1668.
- [4] F. P. Dawalibi, D. Mukhedkar and D. Bensted, "Measured and Computed Current Densities in

- Buried Ground Conductors", IEEE PES 1981 Winter Meeting, Paper # 81 WM 128-8 PWRD.
- [5] F. P. Dawalibi, R. D. Southey and R. S. Baishiki "Validity of Conventional Approaches for Calculating Body Currents Resulting from Electric Shocks", IEEE Trans. on PWRD, Vol. 5, No. 2, April 1990, pp. 613-626.
  - [6] F. P. Dawalibi, W. Xiong and J. Ma, "Effects of Deteriorated and Contaminated Substation Surface Covering Layers on Foot Resistance Calculations", IEEE PES 1992 Winter Meeting, Paper # 92 WM 221-2 PWRD.
  - [7] F. P. Dawalibi and N. Barbeito, "Measurements and Computations of the Performance of Grounding Systems Buried in Multilayer Soils", IEEE Trans. on PWRD, Vol. 6, No. 4, October 1991, pp. 1483-1490.
  - [8] A. B. Oslon and I. N. Stankeeva, "Application of Optical Analogy to Calculation of Electric Fields in Multilayer Media", Electric Technology, U.S.S.R., No. 4, 1979, pp. 68-75.
  - [9] Y. L. Chow, J. J. Yang and K. D. Srivastava, "Grounding Resistance of Buried Electrodes in Multi-Layer Earth Predicted by Simple Voltage Measurements along Earth Surface - A Theoretical Discussion", IEEE/PES 1992 Summer Meeting, Paper # 92 SM 608-0 PWRD.
  - [10] P. J. Lagace, J. L. Houle, Y. Gervais and D. Mukhedkar, "Evaluation of the Voltage Distribution Around Toroidal HVDC Ground Electrodes in N-Layer Soils", IEEE Trans. on PWRD, Vol. 3, No. 4, October 1988, pp. 1573-1577.
  - [11] P. J. Lagace, D. Mukhedkar, H. H. Hoang and H. Greiss, "Evaluation of the the Effect of Vertical Faults on the Voltage Distribution around HVDC Electrodes Using a Supercomputer", IEEE Trans. on PWRD, Vol. 5, No. 3, July 1990, pp. 1309-1313.

#### BIOGRAPHIES

**Dr. Farid Dawalibi (M'72, SM'82)** was born in Lebanon in November 1947. He received a Bachelor of Engineering degree from St. Joseph's University, affiliated with the University of Lyon, and the M.Sc. and Ph.D. degrees from Ecole Polytechnique of the University of Montreal. From 1971 to 1976, he worked as a consulting engineer with the Shawinigan Engineering Company, in Montreal. He worked on numerous projects involving power system analysis and design, railway electrification studies and specialized computer software code development. In 1976, he joined Montel-Sprecher & Schuh, a manufacturer of high voltage equipment in Montreal, as Manager of Technical Services and was involved in power system design, equipment selection and testing for systems ranging from a few to several hundred kV.

In 1979, he founded Safe Engineering Services & technologies, a company which specializes in soil effects on power networks. Since then he has been responsible for the engineering activities of the company including the development of computer software related to power system applications.

He is the author of more than sixty papers on power system grounding and safety, soil resistivity and electromagnetic interference. He has written several research reports for CEA and EPRI.

Dr. Dawalibi is a corresponding member of various IEEE Committee Working Groups, and a senior member of the IEEE Power Engineering Society and the Canadian Society for Electrical Engineering. He is a registered Engineer in the Province of Quebec.

**Dr. Jinxi Ma** was born in Shandong, P.R. China in December 1956. He received the B.Sc. degree in electronics engineering from Shandong University, and the M.Sc. degree in electrical engineering from Beijing University of Aeronautics and Astronautics (BUAA), in 1982 and 1984, respectively. He received the Ph.D. degree in electrical engineering from the University of Manitoba, Winnipeg, Canada in 1991. From 1984 to 1986, he was a research associate with the Dept. of Electrical Engineering, BUAA. He worked on projects involving design and analysis of reflector antennas and calculations of radar cross sections of aircraft.

Since September 1990, he has been with the R & D Department of Safe Engineering Services & technologies, Montreal, Canada. His research interests are in transient electromagnetic scattering and grounding systems in multilayer soils and in soils with finite heterogeneities.

Dr. Ma is a member of IEEE.

**Mr. Robert Southey (M'87)** was born in Shawinigan, Quebec, Canada, on April 26, 1964. He graduated from McGill University, Montreal, in December 1985 with a B. Eng. (Honors) degree in Electrical Engineering.

From that time to the present, he has worked for Safe Engineering Services & technologies, where he is now manager of the Applied R&D Department. of Safe Engineering Services & technologies. He was extensively involved in an EPRI research project investigating electrical interference between pipelines and transmission lines, in a CEA project revising the Canadian Electrical Code section on distribution substation grounding, and in several AC interference studies for gas pipeline construction projects.

Mr. Southey has coauthored several papers on grounding and related subjects. He is a member of IEEE and a registered Professional Engineer in the Province of Quebec.

### Discussion

**D. L. Garrett and F. J. Latham** (Southern Company Services, Birmingham, AL): The authors have provided a useful analysis of the effects of using a multi-layer soil instead of two layers. Mr. Dawalibi's earlier work on parametric analysis of grids in two-layer soils can be used as a basis to show the magnitude of effect the multi-layer model might have. We believe the results of this paper will be very useful, even for those not using a computer program with this capability, to evaluate the impact of frozen soils and substation surfacing material.

To see just how much impact the multi-layer model might have, we analyzed some of the examples in the paper using a two-layer soil model, with the two soil resistivities chosen based on the values of the multi-layer soil model. The results showed that sometimes the impact of the multi-layer model was small, while for other cases it was quite significant.

Some of the results for our two-layer models are shown here:

Figure 1 -  $\rho_1 = 2000 \Omega - m$ ,  $\rho_2 = 100 \Omega - m$ ,  $h = 3m$ ,  $Z = 1.5m$  (Ignore bottom resistivity, grid in upper, high resistivity layer)

current density at conductor extremes = 4.85 (A/m)  
current density at conductor middle = 5.05 (A/m)

For this case, the two-layer model compares well—the bottom, high resistivity layer had little effect.

Figure 1 -  $\rho_1 = 2000 \Omega - m$ ,  $\rho_2 = 100 \Omega - m$ ,  $h = 3m$ ,  $Z = 4.5m$  (ignore bottom resistivity, grid in lower, low resistivity layer)

current density at conductor extremes = 5.15 (A/m)  
current density at conductor middle = 4.96 (A/m)

For this case, the comparison is not as good—the bottom, high resistivity layer has more of an effect because it bounds the low resistivity layer.

Figure 8 -  $\rho_1 = 50 \Omega - m$ ,  $\rho_2 = 1000 \Omega - m$ ,  $h = 3m$  (ignore bottom resistivity)

For  $Z = 1.5m$  (in top layer)—potential at edge = 4.31kV  
potential at center = 5.35kV

The calculated GPR is 5,508 volts.

For  $Z = 4.5m$  (in middle layer)—potential at edge = 4.12kV  
potential at center = 5.3kV

The calculated GPR is 11,165 volts.

For  $Z = 7.5m$  (in bottom layer)—potential at edge = 3.83kV  
potential at center = 4.68kV

The calculated GPR is 12,757 volts.

These results seem to indicate that the grid is significantly affected by lower soil resistivity above or below a grid located in a thin, high resistivity layer. Although the potential as a percent of GPR is not that much different, the absolute value is significantly different. Would it have been more appropriate to ignore the middle layer?

Table 2—grid S4,  $\rho_1 = 100 \Omega - m$ ,  $\rho_2 = 1000 \Omega - m$ ,  $h = 6m$  (assume top resistivity same as middle layer)

For  $Z = 1.5m$  (in top layer) -  $R = 6.15 \Omega$   
For  $Z = 4.5m$  (in middle layer) -  $R = 6.08 \Omega$   
For  $Z = 7.5m$  (in bottom layer) -  $R = 14.20 \Omega$   
For  $Z = 15m$  (deeper in bottom layer) -  $R = 16.58 \Omega$

The most error occurs when the grid is in the ignored layer, as the two-layer model under estimates the resistance for these cases. Once the grid is in the high resistivity layer, the effects of

different resistivity layers above it appear to have negligible affect.

The discussors would like the authors to comment on the following:

For soil models like a or b (three layers), can the bottom layer be ignored without significant error if the grid is in the upper two layers?

For soil models like c or d (five layers), can some kind of average or median values (i.e.,  $\Omega_1 = 150$ ,  $\Omega_2 = 750$ ,  $H = 6$  for soil model d) be used to model a two-layer soil without significant error?

Manuscript received March 1, 1993.

**F. P. DAWALIBI, J. MA, R. D. SOUTHEY:** The authors wish to thank the discussors for their discussion of the paper. Their comments emphasize the inaccuracies which arise when using simplified two-layer soil models instead of multilayer models. In some cases, the inaccuracies are small, while in other cases they are significant.

Question 1 of the discussors refers to the elimination of the bottom layer in soil models like (a) or (b). In most cases, this simplification will cause significant error, while in some cases, the error will be tolerable. For example, when the grid is in the middle layer of soil model (a), ignoring the bottom layer will lead to significant errors in the grounding resistance. When the grid is in the top layer of soil model (b), the error introduced by ignoring the bottom layer will be less significant, especially when the middle layer resistivity is extremely high. Ignoring the middle layer in this soil model when the grid is in the top or middle layer, however, will lead to considerable error (in answer to the question in the middle of the discussion). One other factor to consider is the size of the grounding system. The effect of the bottom layer on the performance of a grounding system is heavily dependent on the size of the grounding system with respect to the total thickness of the layers above the bottom layer. Generally, if the size of the grounding system is small compared to the total layer thickness, the effect of the bottom layer is small. When the size of the grounding system is large compared to the total layer thickness, the effect will be substantial. It should also be noted that a simplified soil model can sometimes give acceptable results for one electric quantity (e.g., grounding resistance) but not for another (e.g., touch voltage).

The answer to Question 2 of the discussors is yes; because in this case the resistivity is monotonically increasing or decreasing, a two-layer soil model can give approximate results without significant error. The accuracy of an equivalent two-layer soil model depends not only on the real multilayer soil itself but also on the size and location of the grounding system, as mentioned above. For example, if a grounding grid is very large, the bottom layer should carry a larger weight in the equivalent soil model. The suggested two-layer soil model  $\rho_1 = 150 \Omega - m$ ,  $h = 6m$  and  $\rho_2 = 750 \Omega - m$  for soil model (d) should be a good approximation for a small or medium sized grid. However, for a large grid whose dimension is many times the total layer thickness, the resistivity of the bottom layer should be higher than  $750 \Omega - m$ .

Manuscript received March 31, 1993.